Comparison of monotonicity challenges encountered by the inverse scattering series and the Marchenko de-multiple method for elastic waves

Reinicke Urruticoechea, C.; Dukalski, M.S.; Wapenaar, C.P.A.

DOI
10.1190/geo2019-0674.1

Publication date
2020

Document Version
Accepted author manuscript

Published in
Geophysics

Comparison of monotonicity challenges encountered by the inverse scattering series and the Marchenko de-multiple method for elastic waves

C. Reinicke*, M. Dukalski† and K. Wapenaar*

ABSTRACT

The reflection response of strongly scattering media often contains complicated interferences between primaries and (internal) multiples, which can lead to imaging artefacts unless handled correctly. Internal multiples can be kinematically predicted, e.g. by the Jakubowicz method or by the inverse scattering series (ISS), as long as monotonicity, i.e. "correct" temporal event ordering, is obeyed. Alternatively, the (conventional) Marchenko method removes all overburden-related wavefield interactions by formulating an inverse problem that can be solved if Green's and so-called focusing functions are separable in the time domain, except for an overlap that must be predicted. For acoustic waves, the assumptions of the aforementioned methods are often satisfied within the recording regimes used for seismic imaging. Elastic media, however, support wave propagation via coupled modes that travel with distinct velocities. Compared to the acoustic case, not only does the multiple issue become significantly more severe, but also violation of monotonicity becomes much more likely. By quantifying the assumptions of the conventional Marchenko method and the ISS, unexpected similarities as well as differences between the requirements of the two methods come to light. Our analysis demonstrates that the conventional Marchenko method relies on a weaker form of monotonicity. However, this advantage must be compensated by providing more prior information, which in the elastic case is an outstanding challenge. Rewriting, or re-mixing, the conventional Marchenko scheme removes the need for prior information but leads to a stricter monotonicity condition, which is now almost as strict as for the ISS. Finally, we present two strategies how the re-mixed Marchenko solutions can be used for imperfect, but achievable, de-multiple purposes.

*Delft University of Technology, Department of Geoscience and Engineering, Stevinweg 1, 2628 CN Delft, The Netherlands. †Aramco Overseas Company B.V., Informaticalaan 6-12, 2628 ZD Delft, The Netherlands.

INTRODUCTION

In seismic exploration, structural images are often derived from a single-sided reflection response. However, traditional imaging methods assume single-scattering reflections (primaries only), such that other events, in particular multiples, create artefacts, which can be significant when the imaging target is buried under a strongly scattering overburden. In elastic media, this problem is worse: each interface couples compressional (P) and shear (S) waves, increasing the number of (unwanted) events drastically. Additionally, due to different propagation speeds of elastic modes, the (converted) primaries associated with an individual reflector arrive at different times, distributing information about this reflector in time. Hence, imaging artefacts can arise not only from (converted) multiples but also from converted primaries, i.e. forward-scattered waves. Reflection data driven methods are not (yet) capable of predicting forward-scattering but they are theorized to be able to handle (converted) multiples.

Wave-equation-based de-multiple methods, such as Jakubowicz (1998), or the inverse scattering series (ISS, Weglein et al., 1997), predict and adaptively subtract internal multiples under two assumptions,

(i) that the temporal ordering of primaries corresponds to the reflector ordering in depth, and

(ii) that internal multiples are recorded after their generating primaries (= primaries associated with the internal multiple generators),

where temporal order refers to vertical travel time. These requirements, known as *monotonicity conditions*, are satisfied for acoustic waves, except for special cases shown by Nita and Weglein (2009). In elastic media, however, violation of monotonicity becomes much easier because of mode conversions (Sun and Innanen, 2019).

A Marchenko-equation-based alternative for *acoustic* waves allows to remove all internal multiples associated with an entire group of layers at once, *without adaptive subtraction* (e.g. Broggini et al., 2012; Wapenaar et al., 2013; Slob et al., 2014).

This method formulates an inverse problem with two equations (derived from reciprocity theorems) and four unknowns: up- and downgoing Green's functions as well as so-called up- and downgoing focusing functions. Numerous studies on the topic feature Green's and focusing functions which are separable in the time domain, except for an unavoidable overlap ($\boldsymbol{\chi}_+$). Given this overlap, two unknowns can be eliminated by muting. Subsequently, two coupled Marchenko equations are obtained and solved for the focusing functions, which once found yield the Green's functions. Eventually, upon multi-dimensional deconvolution of the retrieved Green's functions, overburden-related scattering interactions, including internal multiples, can be removed. We refer to this approach as the *conventional Marchenko method*.

The elastodynamic extension of the Marchenko method bears several challenges. Firstly, speed differences between modes can lead to a second overlap ($\boldsymbol{\chi}_-$), which so far cannot be predicted without knowing the medium and only vanishes conditionally. Secondly, the previously-mentioned unavoidable overlap ($\boldsymbol{\chi}_+$) between Green's and focusing functions is no longer easily predictable without additional constraints, or significantly more prior information (Wapenaar and Slob, 2015). Similar restrictions were encountered by prior work on inverse scattering of coupled modes. Nevertheless, these cases ignored the overlaps, either by assuming sufficiently small velocity differences between modes (Zakharov and Shabat, 1973; Bava and Ghione, 1984), or by excluding coupling (Ware and Aki, 1969).

To overcome the challenge related to the overlap $\boldsymbol{\chi}_+$, we derive a *re-mixed*, as opposed to the above-mentioned *conventional*, Marchenko method: the Green's and focusing functions are transformed such that the unavoidable, highly complex, overlap ($\boldsymbol{\chi}_+$) re-mixes into a trivial one. This strategy can be seen as a combination and generalization of the Marchenko schemes by van der Neut and Wapenaar (2016) and Dukalski et al. (2019).

The Marchenko method uses the aforementioned assumptions about the overlaps to separate the Green's functions from the focusing functions. So far, these requirements have not been sufficiently investigated and have not been compared to the monotonicity conditions of the ISS. Moreover, the requirements of both the Marchenko method and the ISS are only formulated verbally, which makes a direct comparison of the requirements difficult. Therefore, we quantify these assumptions in a form of medium-, angle of incidence and redatuming depth dependent *separability conditions*. This analysis demonstrates that the monotonicity assumptions of the ISS are very similar to, but stricter than, the separability condition of the conventional Marchenko method. After re-mixing, the Marchenko method can be applied without prior medium information (no need for the overlap $\boldsymbol{\chi}_+$). Although, compared to the conventional Marchenko scheme, the separability condition becomes stricter, it still remains slightly more relaxed than the monotonicity assumption (i) of the ISS. This advantage of the (re-mixed) Marchenko method comes from handling the overburden as one complex multiple generator, rather than a stack of independent multiple generators.

Finally, we demonstrate how the solutions of the re-mixed Marchenko method can be used to remove internal multiples, except for internal multiples that predate their generating primaries. In contrast to the ISS, which encounters the same limitation, see assumption (ii), the re-mixed Marchenko method tracks the error caused by the remaining internal multiples. This tracked error is expected to persist in field data studies (e.g. Ravasi et al., 2016; Staring et al., 2018) but could be eliminated by transforming the re-mixed solutions back to the conventional ones, using energy conservation and the minimum-phase property of the focusing function, similar to Dukalski et al. (2019). The latter strategy relies on the reconstruction of a minimum-phase matrix from its normal product, which is subject to ongoing research and will be published elsewhere.

This paper is structured as follows: first, we briefly outline the conventional Marchenko scheme, quantify its assumptions as a separability condition and interpret the required initial estimate. Second, we derive the re-mixed Marchenko scheme, which leads to a stricter separability condition. Third, we quantify monotonicity conditions of the ISS, which we compare to the requirements of the aforementioned (re-mixed) Marchenko method. Finally, we illustrate our findings with numerical examples. In this analysis, we assume surface-related multiples are removed during preprocessing, and thus, use the terms multiples and internal multiples interchangeably. Although we consider the simplest yet non-trivial case, horizontally-layered elastic media, our analysis is already highly relevant for the Middle East (e.g. see El-Emam et al., 2001; Reinicke et al., 2019), and extends qualitatively to more general cases.

Notation

We consider 2D lossless horizontally-layered elastic media in x-z coordinates. According to Snell's law horizontal-slownesses s_x (= horizontal ray-parameter) are conserved,

$$s_x = \frac{\sin\big(\alpha_{p/s}(z)\big)}{c_{p/s}(z)} = \text{constant}, \tag{1}$$

where the subscripts refer to P- and S-waves. Further, $\alpha_{p/s}$ and $c_{p/s}$ are the propagation angle with respect to the vertical axis (z) and the propagation velocity, respectively. A representation in the horizontal-slowness intercept-time (s_x, τ) domain allows to separate 2D wavefields $U(x, z, t)$ into a set of decoupled 1D wavefields,

$$U(s_x, z, \tau) = \int_{-\infty}^{\infty} U(x, z, \tau + s_x x)\mathrm{d}x. \tag{2}$$

In this paper, we use the terms time and intercept-time interchangeably, i.e. the entire analysis considers vertical travel time, *as opposed to* total travel time.

We restrict our analysis to propagating waves, i.e. $|s_x| \leq \frac{1}{c_p}$ (assuming $c_p > c_s$), and neglect measurement-induced limitations, such as a finite bandwidth, because here we wish to focus on a fundamentally physical (not measurement-borne) limitation. Further, we work with P- and S- one-way wavefields (Frasier, 1970; Ursin, 1983), organized in 2×2 matrices

per discrete horizontal-slowness and time,

$$\mathbf{U}(s_x, z, \tau) = \begin{pmatrix} U_{pp} & U_{ps} \\ U_{sp} & U_{ss} \end{pmatrix} (s_x, z, \tau). \tag{3}$$

The elements of the arbitrary wavefield $\mathbf{U}(s_x, z, \tau)$ are associated with source- (second subscript) and receiver-side (first subscript) wavefield potentials (P and S).

Finally, we introduce a detail-hiding notation that omits coordinates and implies temporal convolutions when two matrices $\mathbf{U}_1$ and $\mathbf{U}_2$ are multiplied, for example $\mathbf{U}_1\mathbf{U}_2$ stands for,

$$\int_{-\infty}^{\infty} \mathbf{U}_1(s_x, z, \tau - \tau')\mathbf{U}_2(s_x, z, \tau')\mathrm{d}\tau'. \tag{4}$$

MARCHENKO GREEN'S FUNCTION RETRIEVAL

Suppose all the multiples due to the overburden above the redatuming depth z_i shall be removed. For this purpose, we might use the Green's functions, $\mathbf{G}^{-,+}(s_x, z_0, z_i, \tau)$ and $\mathbf{G}^{-,-}(-s_x, z_0, z_i, \tau)$, associated with down- "+" and upward "−" radiating sources (second superscript) at the redatuming depth z_i, respectively, and recordings of upgoing waves "−" (first superscript) at the acquisition level z_0 (see Fig. 1). From these Green's functions, a redatumed reflection response $\mathbf{R}_{rd}(s_x, z_i, \tau)$, free of overburden-related scattering, can be obtained by solving,

$$\mathbf{G}^{-,+} = -\boldsymbol{\sigma}_z \mathbf{G}^{-,-} \mathbf{R}_{rd}^{\mathrm{T}} \boldsymbol{\sigma}_z, \tag{5}$$

via an Amundsen (2001) deconvolution. Here, we exploit wavefield symmetries in horizontally-layered media via a transpose in P-S space (superscript "T") and via the diagonal matrix, $\boldsymbol{\sigma}_z = \mathrm{diag}\left[\delta(\tau), -\delta(\tau)\right]$, where $\delta(\tau)$ is a temporal delta spike. These symmetries allow us to proceed with the retrieved Green's functions $\mathbf{G}^{-,\pm}$, although they are associated with horizontal-slownesses s_x of opposite sign (a derivation can be found in Appendix A). The challenge is to retrieve these Green's functions from a reflection response $\mathbf{R}(s_x, z_0, \tau)$ recorded at a scattering-free surface z_0 at the top, which can be accomplished by a Marchenko method.

First, we highlight the underlying assumptions and the prior information required by the conventional Marchenko method. Second, we provide a physical interpretation of the prior information, and third, we propose an alternative Marchenko formulation, which trades prior information for stricter assumptions. It will be shown that, both the conventional Marchenko method as well as its alternative formulation rely on separability conditions, which we express quantitatively. In the next section, this quantification will allow us to compare the requirements of the Marchenko method to those of the ISS.

Quantitative separability condition

We briefly outline the elastodynamic Marchenko method, derived by one of the authors (Wapenaar, 2014), and quantify the assumptions as a separability condition.

Instead of predicting multiples by combining all possible triplets of primaries associated with the overburden (Coates and Weglein, 1996), the Marchenko method solves an inverse problem formed by two equations, the convolution- and correlation-type representation theorems,

$$\mathbf{G}^{-,+} \quad + \mathbf{F}_1^- = \mathbf{R}\mathbf{F}_1^+, \tag{6}$$

$$\left(\mathbf{G}^{-,-}\right)^* + \mathbf{F}_1^+ = \mathbf{R}^\dagger \mathbf{F}_1^-, \tag{7}$$

with four unknowns: the Green's functions $\mathbf{G}^{-,\pm}$ and the focusing functions $\mathbf{F}_1^{\pm}(s_x, z_0, z_i, \tau)$. The latter ones are defined in a truncated medium that is identical to the overburden, but scattering-free above z_0 and below z_i. The superscripts denote a time-reversal $(*)$ and a time-reversal combined with a transpose in P-S space (†). Further, an illustration of Eqs. 6-7 can be found in Fig. 1 for an acoustic medium and in Figs. 2a and 3a for an elastic medium.

In an attempt to constrain Eqs. 6-7, two temporal projectors, $\mathbf{P}^{\pm}$, are applied as a Hadamard matrix product in P-S space (details about the projectors can be found in Appendix B). In other publications, the projectors are also referred to as window functions, both terms describe exactly the same thing. Without loss of generality, the projectors preserve the focusing functions, but mute the Green's functions, except for the temporal overlaps, $\mathbf{P}^-\left[\mathbf{G}^{-,+}\right] = \boldsymbol{\chi}_-$ and $\mathbf{P}^+\left[\left(\mathbf{G}^{-,-}\right)^*\right] = \boldsymbol{\chi}_+$, such that Eqs. 6-7 simplify to,

$$\boldsymbol{\chi}_- + \mathbf{F}_1^- = \mathbf{P}^-\left[\mathbf{R}\mathbf{F}_1^+\right], \tag{8}$$

$$\boldsymbol{\chi}_+ + \mathbf{F}_1^+ = \mathbf{P}^+\left[\mathbf{R}^\dagger \mathbf{F}_1^-\right]. \tag{9}$$

Note that, keeping the overlap $\boldsymbol{\chi}_-$ explicit will lead to key insights of this paper. The solution strategy hopes that the overlaps $\boldsymbol{\chi}_\pm$ can be estimated, such that the inverse problem resembles a set of coupled Marchenko equations that can be solved recursively,

$$\mathbf{F}_1^+ = \sum_{k=0}^{\infty} \boldsymbol{\Xi}_k, \text{ with, } \boldsymbol{\Xi}_k = \mathbf{P}^+\left[\mathbf{R}^\dagger \mathbf{P}^-\left[\mathbf{R}\boldsymbol{\Xi}_{k-1}\right]\right], \tag{10}$$

using $\boldsymbol{\Xi}_0 = -\boldsymbol{\chi}_+ - \mathbf{P}^+\left[\mathbf{R}^\dagger \boldsymbol{\chi}_-\right]$ as initial estimate, and assuming convergence of the series (which has been shown for the acoustic case, Dukalski and de Vos, 2017). From the retrieved solution $\mathbf{F}_1^+$, the remaining unknowns can be constructed.

Estimating the overlaps remains very challenging. In order to proceed, the Marchenko method firstly assumes $\boldsymbol{\chi}_-$ is a null matrix $\mathbf{O}$, and secondly, requires $\boldsymbol{\chi}_+$ as prior information (a physical interpretation of $\boldsymbol{\chi}_+$ follows in the next subsection).

The assumption, $\boldsymbol{\chi}_- = \mathbf{O}$, demands that the focusing function $\mathbf{F}_1^-$ and the Green's function $\mathbf{G}^{-,+}$ remain separable in the time domain (see $\mathbf{F}_1^-$/$\mathbf{G}^{-,+}$ separability in Figs. 1a and 2a). Although true for 1.5D acoustic media, this assumption can be violated in 1.5D elastic media (see Fig. 2b), and only holds under the $\boldsymbol{\chi}_-$*-separability-condition*,

$$\sum_{k=1}^{i-1} \Delta z^{(k)} \left(s_{z,s}^{(k)} - s_{z,p}^{(k)}\right) < 2\, \Delta z^{(i)} s_{z,p}^{(i)}, \tag{11}$$

which we derive in Appendix B. Variables $\Delta z^{(k)}$ and $s_{z,p/s}^{(k)}$ denote the thickness and the vertical-slownesses of P- and S-waves in the k^{th} layer, respectively (the layer labelling is depicted in Fig. 5a). The right-hand side of Eq. 11 describes the

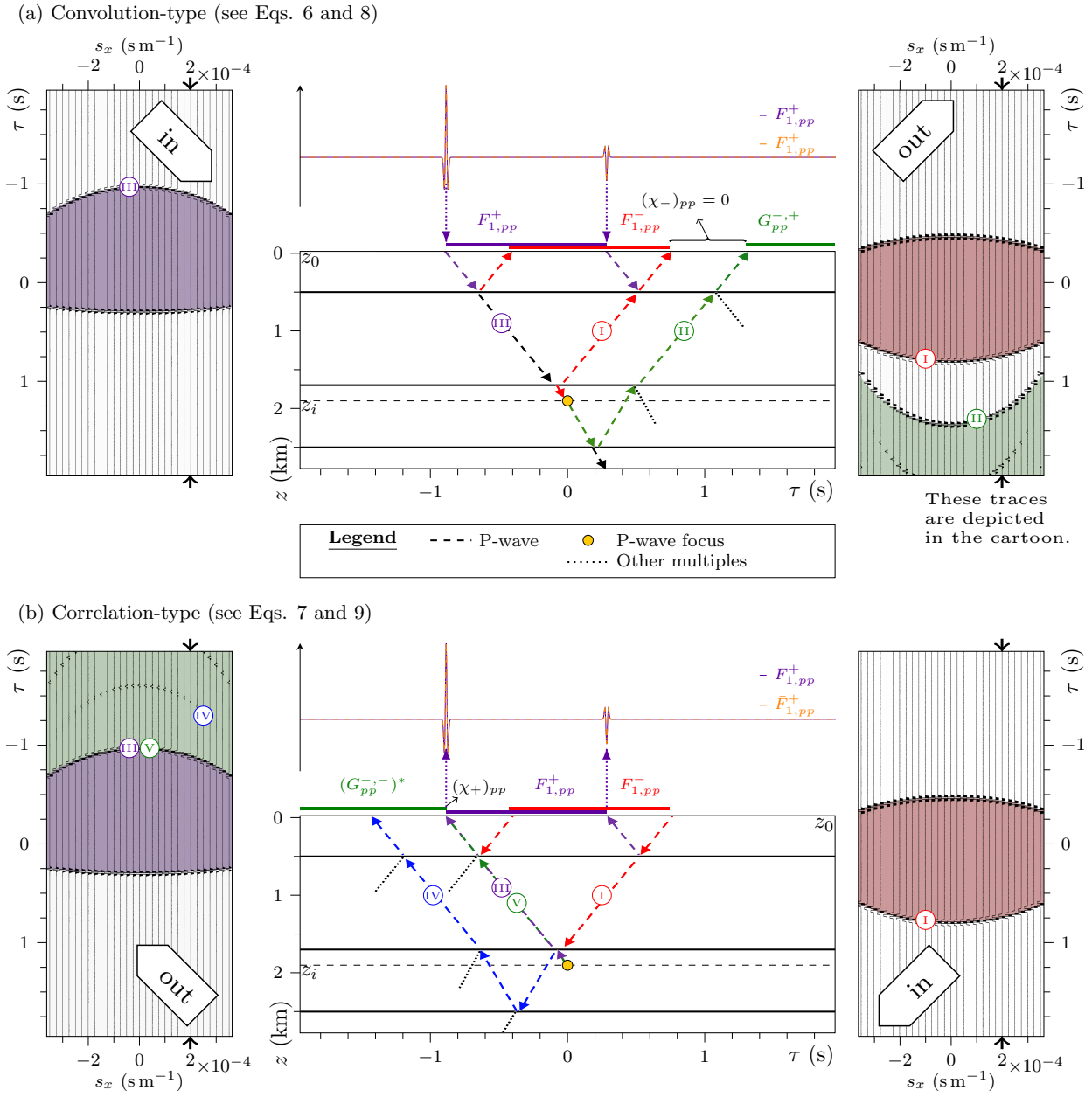

Figure 1: Illustration of the (a) convolution- and (b) correlation-type representation theorems. This figure depicts an acoustic experiment to help the interpretation of the elastic experiments shown in Figs. 2 and 3. The representation theorems describe a scattering experiment: special fields (the focusing functions $\mathbf{F}_1^{\pm}$) are injected into a medium (see arrows saying "in"), the arrow diagram in the centre depicts the scattering paths for a single horizontal-slowness s_x (marked with black arrows in s_x-τ gathers) and another special field scatters back to the recording surface z_0 (see arrows saying "out"). Note that, all wavefields are consistently color-coded in Figs. 1-3. The scattering of $\mathbf{F}_1^+$ (violet in panel a) and $\mathbf{F}_1^-$ (red in panel b) by a (a) time-forwarding and (b) time-reversing medium results in superpositions of focusing and Green's functions, $\mathbf{F}_1^- + \mathbf{G}^{-,+}$ and $\mathbf{F}_1^+ + (\mathbf{G}^{-,-})^*$, respectively. The top trace shows true (violet) and retrieved (orange) focusing functions $F^+_{1,pp}$ and $\bar{F}^+_{1,pp}$, respectively. The last event of $\mathbf{F}_1^-$ (event I) and the first event of $\mathbf{G}^{-,+}$ (event II) are represented by red and green paths, respectively (also see s_x-τ gathers). Similarly, the first event of $\mathbf{F}_1^+$ (event III) and the last event of $(\mathbf{G}^{-,-})^*$ (event V) are highlighted by violet and green travel paths, respectively. The fastest multiple coda of $(\mathbf{G}^{-,-})^*$ (event IV) propagates along the blue path. At the recording surface z_0, the overlap between focusing and Green's functions only contains a direct wave (events III and V). The overlap(s) between focusing and Green's functions appear to have a trivial s_x-dependency (illustrated by the s_x-τ gathers), however, this will change in the elastic case (see Fig. 2). For illustration purposes, all responses are convolved with a 30 Hz Ricker wavelet. Medium parameters can be found in appendix C.

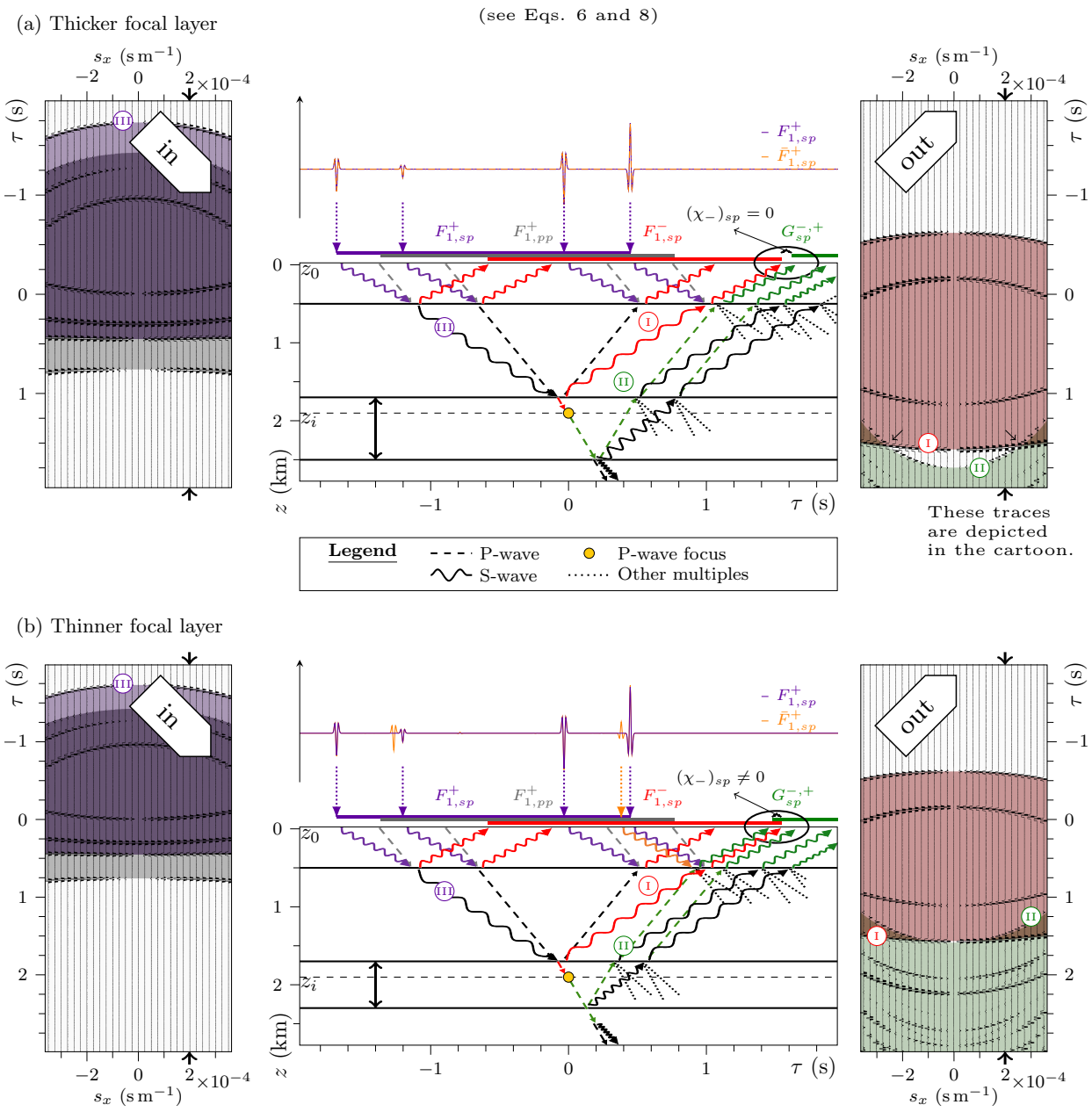

Figure 2: (a) Idem as Fig. 1a for the same medium supporting elastic wave propagation (arbitrarily chosen sp component shown). Compared to the acoustic experiment shown in Fig. 1a, the number of scattering paths increased drastically because at each interface the injected wavefield is reflected and transmitted as P- and S-waves. Moreover, creation of a P-wave focus requires injection of P- (grey color for $F^+_{1,pp}$) and S-waves (violet color for $F^+_{1,sp}$). Due to the mode coupling, the $\mathbf{F}_1^-/\mathbf{G}^{-,+}$ separability is only violated for sufficiently large horizontal-slownesses, $|s_x| > 2.54 \times 10^{-4}\,\mathrm{s\,m^{-1}}$ (indicated by black arrows inside the top-right s_x-τ gather). For smaller horizontal-slownesses, the separability conditions (see Eqs. 11 and 12) are satisfied and the Marchenko method retrieves the correct focusing function (see top trace). (b) Idem as panel (a), except that the thickness of the focusing layer is reduced such that the first event of $G^{-,+}_{sp}$ (event II) predates the last event of $F^-_{1,sp}$ (event I), leading to a temporal overlap (see black ellipse in the cartoon and and red-green area overlap in s_x-τ gathers). If we erroneously assume zero overlap $\boldsymbol{\chi}_- = \mathbf{O}$, the Marchenko method forces the overlapping part of the Green's function to become part of the upgoing focusing function $\bar{\mathbf{F}}_1^-$. As a result, the retrieved downgoing focusing function $\bar{\mathbf{F}}_1^+$ contains an artefact (see orange arrow) that cancels a multiple generated by event II. The other artefacts of the retrieved focusing function $\bar{\mathbf{F}}_1^+$ (e.g. around $\tau = -1.25\,\mathrm{s}$) are caused by similar mechanisms but are not immediately easy to interpret here.

two-way travel time of a P-wave through the i^{th} layer (embedding the redatuming level), and the left-hand side is the one-way travel time difference between a P- and an S-wave propagating from the shallowest to the deepest interface of the overburden. Note that the separability condition becomes stricter if identical projectors, $\mathbf{P}^+ = \mathbf{P}^-$, are used.

Physical interpretation of the overlap $\boldsymbol{\chi}_+$

In 1.5D acoustic media, the overlap $\boldsymbol{\chi}_+$ is a direct wave propagating from the redatuming level z_i to the acquisition surface z_0.

Wapenaar and Slob (2015) demonstrate that, in elastic media, the unavoidable overlap, $\boldsymbol{\chi}_+$, does not simply consist of direct P- and S-waves, but of all waves that forward-scatter from the redatuming level z_i to the acquisition surface z_0 (such as events III and V in Figs. 1b and 3a). This interpretation is a special case. In general, a multiple coda propagating mainly as P-wave may outpace forward-scattered waves propagating mainly as S-waves, e.g. see events IV and III in Fig. 3b, respectively. These multiple coda events become part of the overlap $\boldsymbol{\chi}_+$, and we refer to them as *fast multiples*. The occurrence of fast multiples is prevented if the $\boldsymbol{\chi}_+$*-separability-condition*,

$$\sum_{k=1}^{i-1} \Delta z^{(k)} \left(s_{z,s}^{(k)} - s_{z,p}^{(k)} \right) < 2 \min \left\{ \Delta z^{(k)} s_{z,p}^{(k)} \middle| \, k \in [1,i] \right\}, \tag{12}$$

holds (derived in Appendix B). The minimum function, $\min\{\cdot\}$, selects the smallest element of the given set, which in this case is the delay between the fastest multiple coda and the corresponding forward-scattered wave propagating from z_i to z_0.

If the separability condition in Eq. 12 is violated, the conventional Marchenko method requires the fast multiples as prior information. Even in the special case where Eq. 12 holds such that the overlap $\boldsymbol{\chi}_+$ simplifies to only forward-scattered waves, it still consists of 2^{n-1} events per elastic component, where n is the number of reflectors inside the overburden. Thus, finding the initial estimate $\boldsymbol{\chi}_+$ without further constraints appears very unrealistic for an unknown model.

Marchenko method with trivial initial estimate

In this section, we modify the conventional Marchenko scheme to remove the need for prior information contained by $\boldsymbol{\chi}_+$, in exchange for a stricter separability condition.

We exploit the freedom to convolve the representation theorems in Eqs. 6-7 with an arbitrary time-dependent matrix $\mathbf{B}(s_x, z_i, z_0, \tau)$ from the right,

$$\mathbf{U}^{-,+} \quad + \mathbf{V}_1^- = \mathbf{R}\mathbf{V}_1^+, \tag{13}$$

$$\left(\mathbf{U}^{-,-}\right)^* + \mathbf{V}_1^+ = \mathbf{R}^\dagger \mathbf{V}_1^-, \tag{14}$$

where we introduced $\mathbf{V}_1^\pm = \mathbf{F}_1^\pm \mathbf{B}$, $\mathbf{U}^{-,+} = \mathbf{G}^{-,+}\mathbf{B}$ and $\mathbf{U}^{-,-} = \mathbf{G}^{-,-}\mathbf{B}^*$. This approach allows us to arrive at a different set of equations and can be interpreted as a form of preconditioning (Dukalski and de Vos, 2017). Alike Dukalski et al. (2019), Elison et al. (2020) and Mildner et al. (2019), we assume an unknown, though later recoverable, $\mathbf{B}$, contrary to other authors who use a known $\mathbf{B}$ (van der Neut and Wapenaar, 2016; Meles et al., 2018; Reinicke et al., 2018).

Next, we define the unknown $\mathbf{B}$ such that the overlap $\boldsymbol{\chi}_+$ unfolds onto an identity. This strategy can be seen as applying an unknown transformation (convolution with $\mathbf{B}$) that maps the typically unknown initial guess $\boldsymbol{\chi}_+$ onto a trivial one. As a result, the solutions are also transformed from $\mathbf{F}_1^\pm$ to $\mathbf{V}_1^\pm = \mathbf{F}_1^\pm \mathbf{B}$. We emphasise that the operator $\mathbf{B}$ is not a mere time-shift as in the acoustic scheme by van der Neut and Wapenaar (2016), or a form of a wavelet as in the scheme by Dukalski et al. (2019) and Elison et al. (2020), but a much more general matrix filter. Now Eq. 14 can be easily separated,

$$\mathbf{P}_B^+ \left[\left(\mathbf{U}^{-,-}\right)^* \right] = \boldsymbol{\chi}_+^B = \mathbf{I}, \tag{15}$$

$$\mathbf{P}_B^+ \left[\mathbf{V}_1^+ \right] \quad = \mathbf{V}_1^+, \tag{16}$$

where $\mathbf{I}$ is an identity matrix multiplied by a temporal delta function. Note that the projector $\mathbf{P}_B^+$ can be very different from the projector $\mathbf{P}^+$ in Eq. 9 (details about the projectors can be found in Appendix B). After applying a projector to Eq. 13,

$$\mathbf{P}_B^- \left[\mathbf{U}^{-,+} \right] = \boldsymbol{\chi}_-^B, \tag{17}$$

$$\mathbf{P}_B^- \left[\mathbf{V}_1^- \right] \quad = \mathbf{V}_1^-, \tag{18}$$

we can simplify Eqs. 13 and 14 to,

$$\boldsymbol{\chi}_-^B + \mathbf{V}_1^- = \mathbf{P}_B^- \left[\mathbf{R}\mathbf{V}_1^+ \right], \tag{19}$$

$$\mathbf{I} \quad + \mathbf{V}_1^+ = \mathbf{P}_B^+ \left[\mathbf{R}^\dagger \mathbf{V}_1^- \right]. \tag{20}$$

Compared to Eqs. 8-9, the overlaps $\boldsymbol{\chi}_\pm$ are *re-mixed* into $\boldsymbol{\chi}_-^B$ and $\boldsymbol{\chi}_+^B = \mathbf{I}$, and thus, we refer to $\mathbf{B}$ as the *re-mixing operator*. For the special case that the re-mixed overlap $\boldsymbol{\chi}_-^B$ remains zero we can retrieve re-mixed solutions,

$$\mathbf{V}_1^+ = \sum_{k=0}^{\infty} \boldsymbol{\Xi}_k, \text{ with, } \boldsymbol{\Xi}_k = \mathbf{P}_B^+ \left[\mathbf{R}^\dagger \mathbf{P}_B^- \left[\mathbf{R}\boldsymbol{\Xi}_{k-1} \right] \right], \tag{21}$$

using a trivial initial estimate $\boldsymbol{\Xi}_0 = -\boldsymbol{\chi}_+^B$. Further onwards, we will introduce a de-multiple strategy that only requires the resulting re-mixed Green's functions $\mathbf{U}^{-,\pm}$ as input.

The advantage of a trivial initial estimate, $\boldsymbol{\chi}_+^B = \mathbf{I}$, comes at a cost: although unknown, the re-mixing operator is associated with a source at the surface at z_0 and a receiver at the redatuming depth z_i. Thus, $\mathbf{B}$ moves the focal point to the acquisition surface. This process reduces the temporal separation between the focusing function $\mathbf{F}_1^-$ and the Green's function $\mathbf{G}^{-,+}$ by the temporal extent of the re-mixing operator (see Fig. 4). As a result, an originally zero overlap, $\boldsymbol{\chi}_- = \mathbf{O}$, can become non-zero, $\boldsymbol{\chi}_-^B \neq \mathbf{O}$. This is because the re-mixed Marchenko method relies on the $\boldsymbol{\chi}_-^B$*-separability-condition* (a derivation can be found in Appendix B),

$$\sum_{k=1}^{i-1} \Delta z^{(k)} \left(s_{z,s}^{(k)} - s_{z,p}^{(k)} \right) < \Delta z^{(i)} s_{z,p}^{(i)}, \tag{22}$$

which is stricter than the $\boldsymbol{\chi}_-$-separability-condition of the conventional Marchenko method (see Eq. 11). The effect of satisfying, or violating, the aforementioned separability conditions is summarized in Tab. 1.

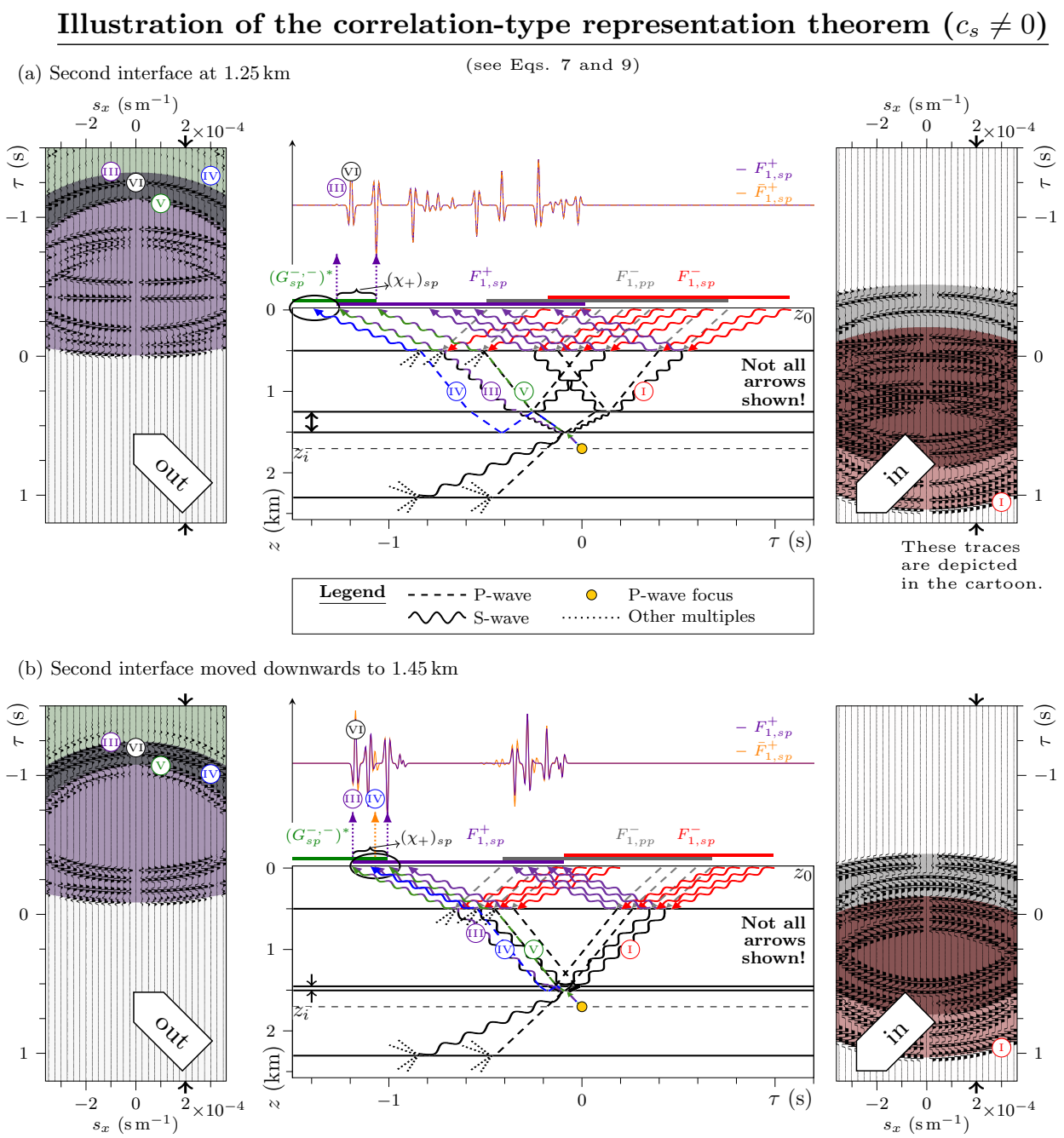

Figure 3: (a) Idem as Fig. 1b but now the medium is elastic and contains an additional interface (arbitrarily chosen sp component shown). Since the additional layer generates so many extra events we do not draw all paths in the cartoon. In contrast to the acoustic case in Fig. 1b, creation of a P-wave focus requires injection of P- (grey color for $F^-_{1,pp}$) and S-waves (red color for $F^-_{1,sp}$). Due to P-S coupling at each interface, the overlap $\boldsymbol{\chi}_+$, which is bounded by the first event of $\mathbf{F}_1^+$ (event III) and the last event of $(\mathbf{G}^{-,-})^*$ (event V), contains not only of a direct wave, but all forward-scattered waves. The s_x-τ gather shows that the temporal separation between forward-scattered waves (e.g. events III, V and VI) and multiples (e.g. event IV) decreases with increasing horizontal-slowness. (b) Idem as panel Fig. 3a, except that the second interface from above has been moved downwards creating a thinner layer (layer thickness reduced from 250 m to 50 m). As a result, the overlap $\boldsymbol{\chi}_+$ contains not only the forward-scattered waves but also fast multiples (see event IV in ellipse). Approximating the overlap $\boldsymbol{\chi}_+$ only by forward-scattered waves, i.e. ignoring fast multiples such as event IV, leads to an erroneous focusing function $\bar{\mathbf{F}}_1^+$ (see orange and violet traces for comparison). Errors occur not only within the temporal extent of the overlap $\boldsymbol{\chi}_+$ but also at other times.

	Separability condition		Satisfied	Violated
Conventional	$\boldsymbol{\chi}_-$ l.h.s. $< 2\,\Delta z^{(i)} s_{z,p}^{(i)}$	(Eq. 11)	$\boldsymbol{\chi}_- = \mathbf{O}$	$\boldsymbol{\chi}_- \neq \mathbf{O}$ with finite duration
	$\boldsymbol{\chi}_+$ l.h.s. $< 2 \min\left\{ \Delta z^{(k)} s_{z,p}^{(k)} \middle\| k \in [1,i] \right\}$	(Eq. 12)	$\boldsymbol{\chi}_+$ *only* contains forward-scattered waves	$\boldsymbol{\chi}_+$ contains forward-scattered waves *and* fast multiples
Re-mixed	$\boldsymbol{\chi}_-^B$ l.h.s. $< \Delta z^{(i)} s_{z,p}^{(i)}$	(Eq. 22)	$\boldsymbol{\chi}_-^B = \mathbf{O}$	$\boldsymbol{\chi}_-^B \neq \mathbf{O}$ with finite duration
	$\boldsymbol{\chi}_+^B$ Unconditionally (by definition $\boldsymbol{\chi}_+^B = \mathbf{I}$)		$\boldsymbol{\chi}_+^B = \mathbf{I}$	not applicable

Table 1: This table summarizes the effect of satisfying, and violating, the separability conditions of the conventional and the re-mixed Marchenko method. The left hand side (l.h.s.) of all inequalities in this table is $\sum_{k=1}^{i-1} \Delta z^{(k)} \left(s_{z,s}^{(k)} - s_{z,p}^{(k)} \right)$.

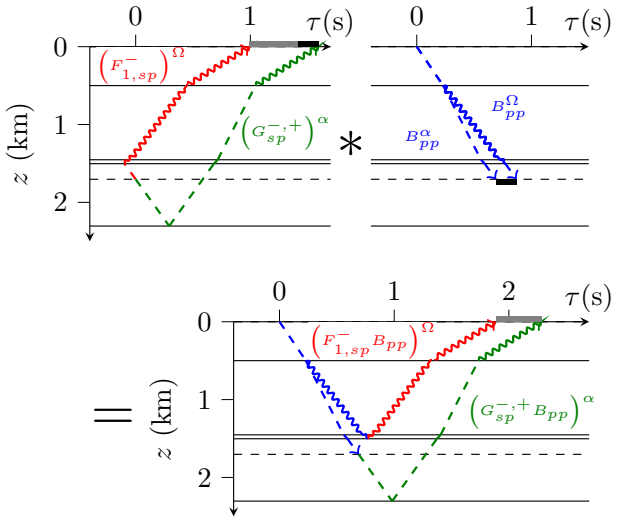

Figure 4: Effect of re-mixing on temporal separation, illustrated analogously to Figs. 2-3. Re-mixing reduces temporal distance between $\mathbf{F}_1^-$ and $\mathbf{G}^{-,+}$ (see grey and black bar) by the duration of the re-mixing operator (see black bar). We depict the first (superscript α) and last (superscript Ω) events of $\mathbf{F}_1^-$ (red), $\mathbf{G}^{-,+}$ (green) and $\mathbf{B}$ (blue). The travel times of the first and the last event of $\mathbf{B}$ are derived in Appendix B.

MONOTONICITY CONDITIONS OF THE ISS

The ISS relies on monotonicity assumptions (i) and (ii) (see *Introduction*), which, to the best of our knowledge, have always been formulated verbally. We quantify these assumptions in a form of two inequalities. Subsequently, we compare them against the conventional and re-mixed Marchenko methods.

Quantifying monotonicity in terms of separability conditions

Consistent with the previous section, we aim to remove multiples related to the overburden above z_i. Monotonicity assumption (i) in the introduction requires that the P-wave travel time through each layer inside the overburden is sufficiently long to separate the (converted) primaries of adjacent reflectors in time (compare Figs. 5a and b), and has to hold for each elastic component. This requirement can be formulated as a separability condition (derived in Appendix B),

$$\sum_{k=1}^{j-1} \Delta z^{(k)} \left(s_{z,s}^{(k)} - s_{z,p}^{(k)} \right) < \Delta z^{(j)} s_{z,p}^{(j)}, \ \forall\, j \in [2,i]. \tag{23}$$

Monotonicity assumption (ii) states that multiples are recorded after their generating primaries and can be formulated as (derived in Appendix B),

$$\sum_{k=1}^{i-1} \Delta z^{(k)} \left(s_{z,s}^{(k)} - s_{z,p}^{(k)} \right) < \min\left\{ \Delta z^{(k)} s_{z,p}^{(k)} \middle\| k \in [1,i] \right\}. \tag{24}$$

Violating monotonicity causes erroneous multiple predictions at the arrival times of primaries (e.g. see Fig. 16 in Sun and Innanen, 2019). Subsequent match-subtraction of the mispredicted multiples may affect the primaries.

Analysis of Marchenko and ISS separability conditions

Now we compare the assumptions of the conventional and re-mixed Marchenko methods (see Eqs. 11, 12 and 22) with the monotonicity assumptions of the ISS (see Eqs. 23 and 24).

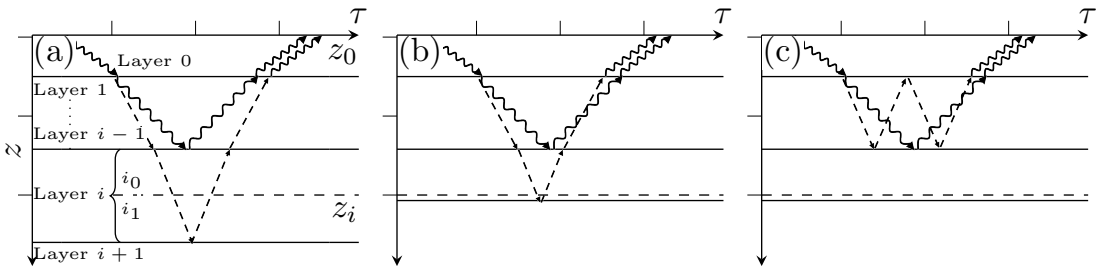

Figure 5: Two primary reflections (arbitrarily chosen ss component) that, (a) obey and (b) violate monotonicity assumption (i). (c) A multiple that predates a primary of one of its generators, violating monotonicity assumption (ii). Dashed and sinusoidal lines represent P- and S-waves, respectively. Layers are labelled with respect to the redatuming depth z_i.

All of the aforementioned methods rely on separability conditions that have the same term on the left-hand side. This term describes the travel time difference between P- and S-waves propagating from the shallowest to the deepest reflector of the overburden. Hence, the likelihood of violating these separability conditions increases with depth and vertical-slowness differences between P- and S-waves ($s_{z,s} - s_{z,p}$).

The re-mixed Marchenko scheme and the ISS can both be evaluated without prior medium information, which makes for a fair comparison: the $\boldsymbol{\chi}_-^B$-separability-condition of the re-mixed Marchenko scheme is nearly identical to the monotonicity assumption (i) of the ISS (compare Eqs. 22 and 23). However, the condition for the re-mixed Marchenko scheme (see Eq. 22) only needs to be obeyed by the redatuming layer i, rather than by each layer inside the overburden (see Eq. 23). For example, a sufficiently slim layer inside the overburden can be prohibitive for the ISS while the re-mixed Marchenko method can handle it, as long as the redatuming layer i provides sufficient temporal support, $\Delta z^{(i)} s_{s,p}^{(i)}$. Hence, the requirement of the re-mixed Marchenko scheme, i.e. the separability of $\mathbf{V}_1^-$ from $\mathbf{U}^{-,+}$, can be seen as a relaxed version of monotonicity condition (i). This advantage of the (re-mixed) Marchenko method can be understood via the fundamentally different nature of the two algorithms: The ISS is applied in a fashion that scans through the data along the time, or (pseudo-)depth, direction, i.e. it treats the medium as a stack of individual multiple generators (although there is *no* need for identifying the generators). In contrast, the (re-mixed) Marchenko method exploits scattering relations between wavefields associated with a shallow and a deep part of the medium, where the separation between shallow and deep is arbitrary (Dukalski and De Vos, 2020). Once retrieved, these wavefields can be used to remove multiples generated by the shallow medium (=the overburden). Thus, the overburden is handled as one complex multiple generator.

The $\boldsymbol{\chi}_-$-separability-condition of the conventional Marchenko method is more relaxed (compare Eqs. 11, 22 and 23). This relaxation emerges due to a missing factor of two on the left-hand side of Eq. 11, i.e. the conventional Marchenko scheme demands temporal separability in terms of one- instead of two-way travel time ($\mathbf{F}_1^- \leftrightarrow \mathbf{V}_1^-$ and $\mathbf{G}^{-,+} \leftrightarrow \mathbf{U}^{-,+}$). However, the more relaxed separability condition must be compensated by estimating the remaining overlap $\boldsymbol{\chi}_+$, i.e. by providing prior information. Hence, the re-mixed Marchenko method trades prior information for a stricter assumption. This trade-off was not discussed by van der Neut and Wapenaar (2016) because they did not consider forward-scattered waves.

Further, elastic overburden removal via the ISS entails a high risk of violating the monotonicity assumption (ii), which is quantified by Eq. 24: with increasing depth the right-hand side of the condition decreases or remains constant, while the left-hand side increases. In other words, increasing depth leads to a higher probability of fast multiples occurring, i.e. multiples outpacing their generating primaries. Fast multiples can also be encountered by the conventional Marchenko method, which requires them to be included in the initial estimate. Again, due to one- and two-way travel times, the occurrence of fast multiples in the conventional Marchenko method and the ISS differs by a factor of two (compare Eqs. 12 and 24). The re-mixed Marchenko scheme encodes the effect of fast multiples in the re-mixing operator $\mathbf{B}$, which allows us to solve the scheme with a trivial initial estimate. However, the re-mixing operator remains in the retrieved solutions ($\mathbf{V}_1^{\pm}$ and $\mathbf{U}^{-,\pm}$). Hence, the re-mixed Marchenko scheme tracks, but does not remove, the impact of fast multiples (which will become obvious in Eq. 26 in the next section).

Note that the discussed separability conditions only consider the temporal event ordering, but neglect the amplitudes of the events. Errors due to violating the separability conditions may be negligible close to zero-incidence where mode conversions are weak, but become increasingly significant with increasing angle of incidence.

Moreover, the separability conditions are domain-dependent. Among others, Sun and Innanen (2016) have addressed this issue in the context of the ISS. For Marchenko methods, the separation of focusing functions from the Green's functions is typically performed in the space-time (e.g. Wapenaar et al., 2014) or in the linear Radon domain (e.g. Slob et al., 2014). The separation in the latter domain is favorable, particularly in 1.5D media, because horizontal-slownesses can be treated separately, reducing the risk of unwanted overlaps. It may be possible to relax the separability conditions further by considering another domain, which will be subject to future investigation.

DE-MULTIPLE STRATEGIES FOR RE-MIXED MARCHENKO SCHEME

Now we propose two de-multiple strategies derived from the re-mixed Marchenko solutions. The first one only requires the re-mixed solutions but does not remove all overburden interactions. The second one aims to remove all overburden interactions by exploiting energy conservation and the minimum-phase property of the focusing function. The latter approach is discussed only conceptually and may enable the recovery of the focusing function $\mathbf{F}_1^+$, which will be discussed further in the future.

Re-mixed Marchenko de-multiple method

The two Green's functions $\mathbf{G}^{-,\pm}$ are related by the redatumed reflection response $\mathbf{R}_{rd}$ (see Eq. 5), that is free of overburden interactions, and thus, is a form of overburden-borne multiple and forward-scattering elimination. In contrast, the re-mixed Green's functions $\mathbf{U}^{-,\pm}$ are mutually related by a target reflection response $\mathcal{R}$,

$$\mathbf{U}^{-,+} = -\boldsymbol{\sigma}_z \mathbf{U}^{-,-} \mathcal{R}, \tag{25}$$

which can be retrieved via deconvolution (still per horizontal-slowness s_x). By inserting an identity, $\mathbf{B}^* \left(\mathbf{B}^*\right)^{-1}$, in Eq. 5, multiplying the result by $\mathbf{B}$ from the right, and using the definitions of the re-mixed Green's functions (see below Eq. 14), we see that the target response $\mathcal{R}$ is related to the redatumed reflection response $\mathbf{R}_{rd}$,

$$\mathcal{R} = \left(\mathbf{B}^*\right)^{-1} \mathbf{R}_{rd}^{\mathrm{T}} \boldsymbol{\sigma}_z \mathbf{B}. \tag{26}$$

In this process, we introduced a convolutional and matricial, more general, Moore-Penrose pseudo-inverse of $\mathbf{B}$, denoted by the superscript "-1". Even though in our numerical experiments $\mathbf{B}$ was always invertible, we currently cannot offer any proof to assume invertibility in general. Moreover, for band-limited signals the matrix inverse does not exist outside the spectral band of the signal, analogously to wavelet deconvolution. Unlike the Green's function $\mathbf{G}^{-,\pm}$, the re-mixed ones are easily calculable provided that the separability condition Eq. 22 holds. The target reflection response $\mathcal{R}$ (see Eq. 26) is the desired redatumed reflection response, dressed with all overburden interactions described by $\mathbf{B}$ on the source- and receiver-sides. In a 1.5D acoustic case, $\mathbf{B}$ commutes with the redatumed reflection response $\mathbf{R}_{rd}$ and the product $\left(\mathbf{B}^*\right)^{-1} \mathbf{B}$ cancels except for a time-shift defined by the overburden. However, in 2D, this is no longer the case. In the elastic situation, in the absence of fast multiples (see Eq. 12) $\mathbf{B}$ is an inverse time-reversed forward-scattered transmission through the overburden. This insight ties back to the statement in the introduction that forward-scattering cannot be predicted by existing methods. If Eq. 12 is violated, $\mathbf{B}$ also carries the imprint of fast multiples (e.g. see Fig. 6 and Fig. 7 in Appendix D).

Moreover, the impact of forward-scattering and fast multiples can be understood and tracked via the re-mixing operator (see Eq. 26). If the re-mixing operator can be retrieved, the aforementioned errors could even be corrected. This convenience is possible because the (re-mixed) Marchenko method only relies on linear scattering relations between fields defined in the overburden-only and fields defined in the entire medium. In contrast, de-multiple schemes that predict multiples only kinematically do not yet offer the opportunity to track the above-mentioned errors.

Alternative de-multiple strategy

We conjecture it could be possible to remove all overburden interactions, including forward-scattering and (fast) multiples, by exploiting further physical constraints: energy conservation and the minimum-phase property of the focusing function. In the following, we make the first steps in this direction.

The up- and downgoing focusing functions conserve energy,

$$\left(\mathbf{F}_1^+\right)^\dagger \mathbf{F}_1^+ - \left(\mathbf{F}_1^-\right)^\dagger \mathbf{F}_1^- = \mathbf{I}, \tag{27}$$

i.e. the net energy injected at z_0 equals the transmitted energy at z_i - a delta source at time zero. Firstly, by evaluating energy conservation of the re-mixed focusing function, $\mathbf{V}_1^\pm = \mathbf{F}_1^\pm \mathbf{B}$, and using Eq. 27, we obtain the normal product of the re-mixing operator,

$$\left(\mathbf{F}_1^+\mathbf{B}\right)^\dagger \mathbf{F}_1^+\mathbf{B} - \left(\mathbf{F}_1^-\mathbf{B}\right)^\dagger \mathbf{F}_1^-\mathbf{B} = \mathbf{B}^\dagger\mathbf{B}. \tag{28}$$

Secondly, we find a convolutional and matricial Moore-Penrose pseudo-inverse of $\mathbf{B}^\dagger\mathbf{B}$, and convolve the result by the re-mixed focusing function $\mathbf{V}_1^+$ from the left and right,

$$\mathbf{F}_1^+\mathbf{B}\left(\mathbf{B}^\dagger\mathbf{B}\right)^{-1}\left(\mathbf{F}_1^+\mathbf{B}\right)^\dagger = \mathbf{F}_1^+\left(\mathbf{F}_1^+\right)^\dagger. \tag{29}$$

The result is the normal product of the desired focusing function $\mathbf{F}_1^+$ and can be seen as a generalized power spectrum. Note that, Eqs. 27-29 also hold for band-limited wavefields. If the focusing function $\mathbf{F}_1^+$ can be retrieved from its normal product $\mathbf{F}_1^+\left(\mathbf{F}_1^+\right)^\dagger$, the desired Green's functions and hence the redatumed reflection response $\mathbf{R}_{rd}$, free of all overburden interactions, can be obtained (from Eq. 5).

We aim to retrieve the focusing function $\mathbf{F}_1^+$ from its normal product using a physical constraint. The focusing function $\mathbf{F}_1^+$ is an inverse of a transmission response. In 1D acoustics, this relation implies that the focusing function is a minimum-phase scalar function, except for a linear phase-shift, and hence, possesses a unique amplitude-phase relationship via the Kolmogorov relation (Claerbout, 1985). This property allows Dukalski et al. (2019) and Elison et al. (2020) to factorize the (scalar) normal product $\mathbf{F}_1^+\left(\mathbf{F}_1^+\right)^\dagger$, and thereby, predict short-period multiples that are generated in a horizontally-layered acoustic overburden. In our case, the focusing function as a matrix is still an inverse transmission, and therefore, remains a minimum-phase object in a matrix sense. Tunnicliffe-Wilson (1972) proposes a method that factorizes the normal products of a sub-class of minimum-phase matrices. The generalization of this method is subject of ongoing research and will be published in the future. If this strategy can be successfully implemented, there is no need to retrieve the unknown operator $\mathbf{B}$. For an interested reader, however, we still present a numerical example of $\mathbf{B}$ in Appendix D.

NUMERICAL EXAMPLES

For horizontally-layered media, all required wavefields can be modelled efficiently by wavefield extrapolation without band-limitation (Kennett and Kerry, 1979; Hubral et al., 1980). Further, we choose the P- and S-wave velocities as well as the horizontal-slownesses such that all events are on-sample, i.e. the arrival times of all events are integer multiples of the temporal sampling interval (medium parameters are specified in Appendix C). This allows us to better inspect the separability conditions of the conventional and re-mixed Marchenko methods because measurement-induced limitations are absent.

First, we consider the experiment in Fig. 2a that satisfies the $\boldsymbol{\chi}_-$-separability-condition of the conventional Marchenko method stated by Eq. 11. Using the correct initial estimate $\boldsymbol{\chi}_+$, which is obtained by applying the projector $\mathbf{P}^+$ (defined in Appendix B) to a modelled Green's function (i.e. the medium is known a-priori), the elastodynamic Marchenko method finds the correct focusing function (see trace in Fig. 2a). However, when repeating this experiment for the model in Fig. 2b, which violates the $\boldsymbol{\chi}_-$-separability-condition in Eq. 11, the projector $\mathbf{P}^-$ erroneously preserves the first event of $\mathbf{G}^{-,+}$ (event II). Assuming, $\boldsymbol{\chi}_- = \mathbf{O}$, forces this event to become part of the focusing function $\bar{\mathbf{F}}_1^-$ (the bar distinguishes retrieved from true solutions). To cancel multiples caused by this event, the retrieved $\bar{\mathbf{F}}_1^+$ contains an artefact (see orange arrow in Fig. 2b). Via the same mechanism, further artefacts are introduced.

Second, for the experiment shown in Fig. 3a, which still satisfies the $\boldsymbol{\chi}_-$-separability-condition in Eq. 11 as well as the $\boldsymbol{\chi}_+$-separability-condition in Eq. 12, the Marchenko series (see Eq. 10) finds the correct solution (see trace in Fig. 3a), using the forward-scattered part of the Green's function $(\mathbf{G}^{-,-})^*$ as initial estimate. By downward-shifting the second interface, as depicted in Fig. 3b, Eq. 12 is violated and the overlap $\boldsymbol{\chi}_+$ is populated with fast multiples. If the initial estimate ignores these fast multiples, the Marchenko series does not converge to the true solution. For example, event IV, which is a (fast) multiple belonging to the Green's function, is now (erroneously) part of the focusing function (indicated by the orange-dotted line in Fig. 3b). To compensate for these errors the Marchenko series introduces further artefacts (particularly see errors after $t = -0.6\,\mathrm{s}$ in Fig. 3b).

Third, we repeat the previous experiment with the re-mixed Marchenko scheme, which simplifies the highly sophisticated initial estimate $\boldsymbol{\chi}_+$ to a trivial one $\boldsymbol{\chi}_+^B = \mathbf{I}$. We use the re-mixed solutions to remove multiples according Eq. 26. Since there is only one reflector below the redatuming level one would hope to eliminate all scattering effects except for a single primary (event A in Fig. 6). Indeed, a significant amount of overburden interactions has been removed, revealing the primary A, which was masked by a strong multiple (see traces and cartoon in Fig. 6). Nevertheless, the redatumed response still contains forward-scattered waves (e.g. events B and D) as well as fast multiples (e.g. event C). These remaining scattering effects are caused by re-mixing. The corresponding operator ($\mathbf{B}$) is angle-dependent because it is implicitly defined by the overlap $\boldsymbol{\chi}_+$ (see s_x-τ gathers in Fig. 3, for an explicit example see Appendix D). Following the alternative de-multiple strategy, that aims to remove all overburden interactions, we can already recover the normal product of the desired focusing function $\mathbf{F}_1^+$ near-to-perfectly (no figure), with a relative error below $1\,\mathrm{ppm}$ (for the model in Figs. 3b and 6). Experiments on retrieving the focusing function from its normal product are beyond the scope of this paper.

CONCLUSION

Our analysis revealed that the conventional Marchenko method, similarly to the ISS, relies on a form of monotonicity, but in terms of one- instead of two-way travel time. The former one is a less restrictive condition. However, this advantage of the conventional Marchenko method must be compensated by providing an initial estimate, i.e. prior information, which becomes challenging in practice. To remove the need for prior information, we introduced the re-mixed Marchenko scheme, which allows for a fair comparison with the requirements of the ISS. The re-mixed Marchenko scheme still relies on a less restrictive form of monotonicity than the ISS because it only requires the redatuming layer, instead of each layer in the overburden, to be sufficiently thick (in terms of P-wave travel time). Through this comparison, we gained significant insights about challenges of the elastic de-multiple problem. We believe that these advances, and addressing the problems raised in this paper, are essential for further development of a full elastic Marchenko method.

Moreover, we presented two strategies how the re-mixed Marchenko equations can be used for multiple elimination. The first one can be easily implemented and removes all multiples that arrive after their generating primaries. The second strategy aims to remove all overburden-related effects, including forward-scattering and (fast) multiples, by removing the re-mixing operator from the Marchenko solutions. For this purpose, additional physical constraints are taken into account, namely energy conservation and the minimum-phase property of the (delayed) focusing function. The latter constraint is often associated with wavelets but it is in fact a property of an entire wavefield, which we propose to exploit. Using a minimum-phase constraint for the prediction of forward-scattered waves and fast multiples requires minimum-phase matrix factorization, which is subject to ongoing research.

ACKNOWLEDGMENTS

This work was supported by the European Union's Horizon 2020 research and innovation programme: Marie Sklodowska-Curie [grant number 641943] and European Research Council [grant number 742703]. We would like to thank Kris Innanen and Dirk-Jan van Manen for reviewing and helping to improve this paper.

APPENDIX A: DERIVATION OF THE REDATUMING RELATION

In this appendix, we derive the expression in Eq. 5 that relates the redatumed reflection response $\mathbf{R}_{rd}(s_x, z_i, \tau)$ to the retrieved Green's functions $\mathbf{G}^{-,\pm}(\pm s_x, z_0, z_i, \tau)$. For this deriva-

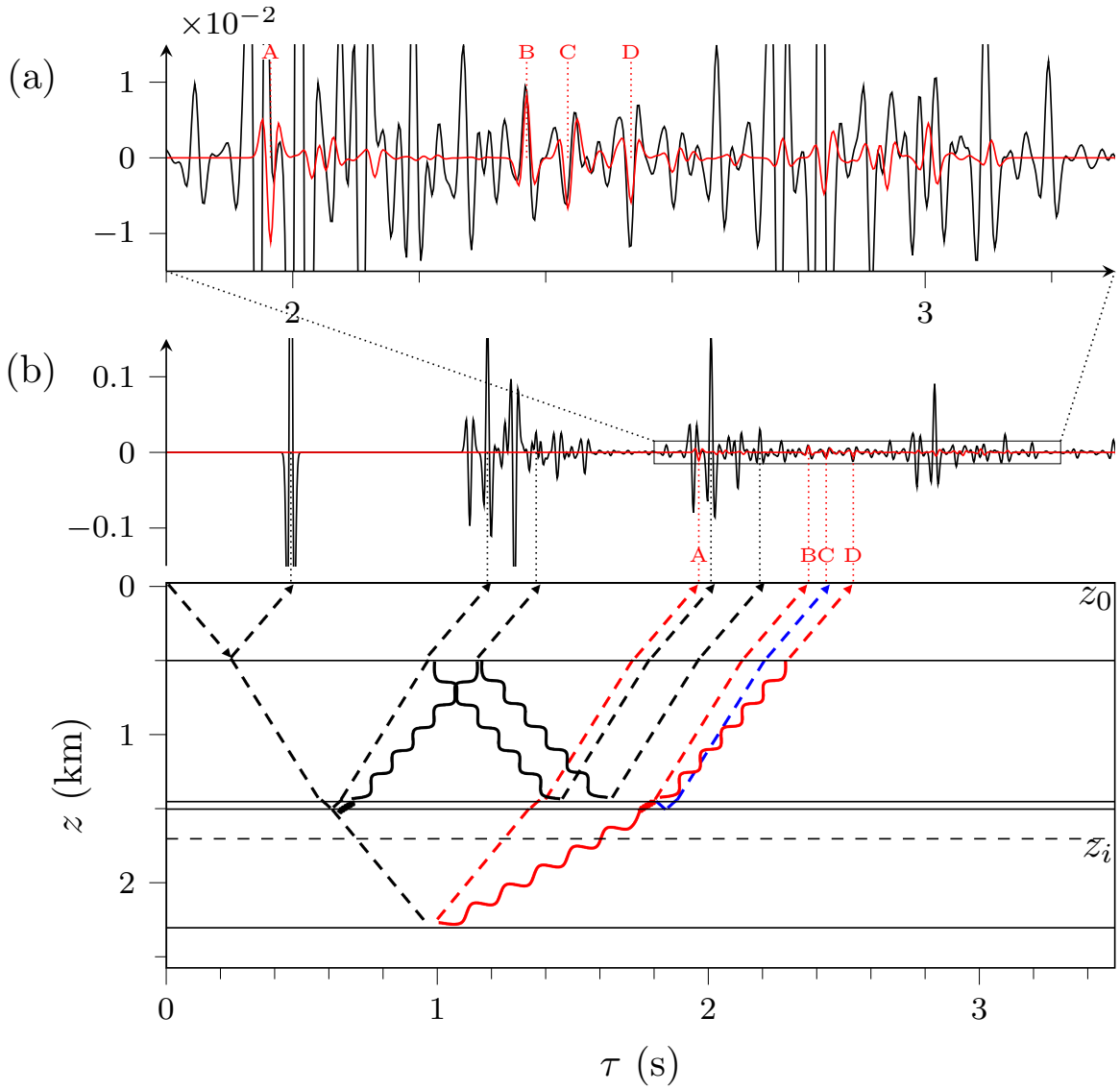

Figure 6: Reflection response (black traces) and de-multiple result (red traces) according to Eq. 26 (arbitrarily chosen *pp* component, $s_x = 2 \times 10^{-4}\,\mathrm{s\,m^{-1}}$). Panel (a) shows a close-up of the box in panel (b). Again, dashed and sinusoidal lines represent P- and S-waves, respectively. The cartoon highlights (1) some of the overburden interactions removed by the de-multiple scheme (black lines), and (2) the four strongest events remaining in the redatumed result (red and blue lines): event A is the desired target-related primary reflection, events B and D are forward-scattered waves, and event C (highlighted in blue) is a fast multiple. Dotted lines point to the arrivals associated with the cartoon arrows. For illustration purposes, all responses are convolved with a 30 Hz Ricker wavelet and a global scaling factor is used to adjust the de-multiple result to the reflection response.

tion, we write all coordinates explicitly, but matrix products still imply temporal convolutions according to Eq. 4.

The starting point is the more familiar redatuming relation,

$$\mathbf{G}^{-,+}(s_x,z_i,z_0,\tau)=\mathbf{R}_{rd}(s_x,z_i,\tau)\mathbf{G}^{+,+}(s_x,z_i,z_0,\tau). \tag{A-1}$$

Next, we use source-receiver reciprocity (e.g. see Wapenaar, 2014),

$$\mathbf{G}^{\mp,+}(s_x,z_i,z_0,\tau)=\pm\left[\mathbf{G}^{-,\pm}(-s_x,z_0,z_i,\tau)\right]^{\mathrm{T}}, \tag{A-2}$$

and to interchange source and receiver in Eq. A-1,

$$\begin{aligned}\mathbf{G}^{-,+}(s_x,z_0,z_i,\tau)&=\left[\mathbf{G}^{-,+}(-s_x,z_i,z_0,\tau)\right]^{\mathrm{T}}\\&=\left[\mathbf{G}^{+,+}(-s_x,z_i,z_0,\tau)\right]^{\mathrm{T}}\left[\mathbf{R}_{rd}(-s_x,z_i,\tau)\right]^{\mathrm{T}}\\&=-\mathbf{G}^{-,-}(s_x,z_0,z_i,\tau)\left[\mathbf{R}_{rd}(-s_x,z_i,\tau)\right]^{\mathrm{T}}.\end{aligned} \tag{A-3}$$

In horizontally-layered media, wavefields associated with positive and negative horizontal-slownesses s_x are mutually related via multiplication by a Pauli matrix $\boldsymbol{\sigma}_z$ (multiplied by a temporal delta spike) from the left and right, which yields,

$$\begin{aligned}&\mathbf{G}^{-,+}(s_x,z_0,z_i,\tau)=\\&\quad=-\boldsymbol{\sigma}_z\mathbf{G}^{-,-}(-s_x,z_0,z_i,\tau)\boldsymbol{\sigma}_z\boldsymbol{\sigma}_z\left[\mathbf{R}_{rd}(s_x,z_i,\tau)\right]^{\mathrm{T}}\boldsymbol{\sigma}_z\\&\quad=-\boldsymbol{\sigma}_z\mathbf{G}^{-,-}(-s_x,z_0,z_i,\tau)\left[\mathbf{R}_{rd}(s_x,z_i,\tau)\right]^{\mathrm{T}}\boldsymbol{\sigma}_z.\end{aligned} \tag{A-4}$$

APPENDIX B: DERIVATION OF SEPARABILITY CONDITIONS

In this appendix, we formulate the separability conditions of the ISS, and of the original as well as the re-mixed representation theorems. Furthermore, we derive explicit expression of the projectors $\mathbf{P}^{\pm}$ and $\mathbf{P}_B^{\pm}$.

Consider a homogeneous layer (labelled by k) of thickness $\Delta z^{(k)}$ as well as P- and S-wave velocities $c_p^{(k)}$ and $c_s^{(k)}$. For a plane wave with horizontal slowness s_x, P- and S-waves propagate with the vertical slowness,

$$s_{z,p/s}^{(k)}=\sqrt{\left(c_{p/s}^{(k)}\right)^{-2}-s_x^2}. \tag{B-1}$$

The resulting one-way travel time of such plane waves through layer k is,

$$\tau_{p/s}^{(k)}=\Delta z^{(k)}s_{z,p/s}^{(k)}. \tag{B-2}$$

In the following, we assume that the P-wave velocity,

$$c_p=\sqrt{\frac{\lambda+2\mu}{\rho}}, \tag{B-3}$$

is greater than the S-wave velocity,

$$c_s=\sqrt{\frac{\mu}{\rho}}, \tag{B-4}$$

de Hoop (1995), which is the case for most materials: The shear modulus μ and the density ρ are always positive. The first Lamé parameter λ can be negative but for all natural materials known to the authors the relation $\lambda>-\mu$ holds.

Appendix B1: Separability of conventional representation theorems

In the following, we derive the separability conditions implied by the conventional Marchenko scheme.

First, we analyze the separability of the focusing function $\mathbf{F}_1^-$ from the Green's function $\mathbf{G}^{-,+}$ on the left-hand side of Eq. 6. To guarantee separability, the last and first events of the focusing and Green's functions must satisfy the condition,

$$\tau_\Omega(F_{1,ab}^-)<\tau_\alpha(G_{ab}^{-,+}), \tag{B-5}$$

for each elastic component combination ab. Here, the functions τ_α and τ_Ω denote the first and last arrival times at the recording level z_0, respectively. We sum the one-way travel times along the travel path of the last event of $F_{1,ab}^-$ (e.g. for $F_{1,sp}^-$ see event I in Fig. 2a, see Fig. 5 for layer labelling $i_{0/1}$),

$$\tau_\Omega(F_{1,ab}^-)=\tau_a^{(0)}+\sum_{k=1}^{i-1}\tau_s^{(k)}-\tau_b^{(i_0)}, \tag{B-6}$$

and along the travel path of the first event of $G_{ab}^{-,+}$ (e.g. for $G_{sp}^{-,+}$ see event II in Fig. 2a),

$$\tau_\alpha(G_{ab}^{-,+})=\tau_a^{(0)}+\sum_{k=1}^{i}\tau_p^{(k)}+\tau_b^{(i_1)}. \tag{B-7}$$

We substitute Eqs. B-6 and B-7 in Eq. B-5, replace the one-way travel times by Eq. B-2 and obtain the $\boldsymbol{\chi}_-$-separability-condition of Eq. 11,

$$\sum_{k=1}^{i-1}\Delta z^{(k)}\left(s_{z,s}^{(k)}-s_{z,p}^{(k)}\right)<2\,\Delta z^{(i)}s_{z,p}^{(i)}. \tag{B-8}$$

Second, we derive a condition under which the overlap $\boldsymbol{\chi}_+$ simplifies to the forward-scattered part of the Green's function $\left(\mathbf{G}^{-,-}\right)^*$. This scenario requires that the fastest multiple coda of the (time-reversed) Green's function $\left(\mathbf{G}^{-,-}\right)^*$ reaches the recording level before the first event of the focusing function $\mathbf{F}_1^+$ (which defines the first event of the overlap $\boldsymbol{\chi}_+$),

$$\tau_\Omega\left((G_{m,ab}^{-,-})^*\right)<\tau_\alpha(F_{1,ab}^+). \tag{B-9}$$

Here, we use the subscript m to refer to the multiples of a wavefield. We sum the one-way travel times along the path of the fastest multiple coda of the Green's function $\left(G_{m,ab}^{-,-}\right)^*$ (e.g. for $(G_{m,sp}^{-,-})^*$ see event IV in Fig. 3a),

$$\begin{aligned}&\tau_\Omega((G_{m,ab}^{-,-})^*)=\\&-\tau_a^{(0)}-\sum_{k=1}^{i-1}\tau_p^{(k)}-2\,\min\left\{\tau_p^{(k)}\,\middle|\,k\in[1,i]\right\}-\tau_b^{(i_0)},\end{aligned} \tag{B-10}$$

and along the travel path of the first event of the focusing function $F_{1,ab}^+$ (e.g. for $F_{1,sp}^+$ see event III in Fig. 3a),

$$\tau_\alpha(F_{1,ab}^+)=-\tau_a^{(0)}-\sum_{k=1}^{i-1}\tau_s^{(k)}-\tau_b^{(i_0)}. \tag{B-11}$$

We substitute Eqs. B-10 and B-11 in Eq. B-9, express the one-way travel times according to Eq. B-2 and arrive at the $\boldsymbol{\chi}_+$-separability-condition,

$$\sum_{k=1}^{i-1} \Delta z^{(k)} \left(s_{z,s}^{(k)} - s_{z,p}^{(k)} \right) < 2 \min \left\{ \Delta z^{(k)} s_{z,p}^{(k)} \middle| \, k \in [1,i] \right\}. \tag{B-12}$$

This condition can only be satisfied if the separability condition in Eq. B-8 holds.

If the separability condition in Eq. B-8 holds the projector $\mathbf{P}^-$, acting as a Hadamard matrix product in P-S space, separates the convolution-type representation theorem in Eq. 6 according to,

$$\mathbf{P}^- \left[\mathbf{G}^{-,+} \right] = \boldsymbol{\chi}_- = \mathbf{O}, \tag{B-13}$$

$$\mathbf{P}^- \left[\mathbf{F}_1^- \right] = \mathbf{F}_1^-. \tag{B-14}$$

We define the projector $\mathbf{P}^-$ such that all events after the last arrival of the focusing function $\mathbf{F}_1^-$ are muted,

$$\begin{aligned} P_{ab}^- &= \mathrm{H}\left(-\tau + \tau_\Omega(F_{1,ab}^-) \right) \\ &= \mathrm{H}\left(-\tau + \tau_a^{(0)} + \sum_{k=1}^{i-1} \tau_s^{(k)} - \tau_b^{(i_0)} \right), \end{aligned} \tag{B-15}$$

where we use Eq. B-6. The function $\mathrm{H}(\tau)$ denotes the Heaviside function, $\mathrm{H}(\tau < 0) = 0$ and $\mathrm{H}(\tau \geq 0) = 1$. In analogy, the correlation-type representation theorem in Eq. 7 can be separated with a projector $\mathbf{P}^+$,

$$\mathbf{P}^+ \left[(\mathbf{G}^{-,-})^* \right] = \boldsymbol{\chi}_+, \tag{B-16}$$

$$\mathbf{P}^+ \left[\mathbf{F}_1^+ \right] = \mathbf{F}_1^+, \tag{B-17}$$

that mutes all events before the first arrival of the focusing function $\mathbf{F}_1^+$,

$$\begin{aligned} P_{ab}^+ &= \mathrm{H}\left(\tau - \tau_\alpha(F_{1,ab}^+) \right) \\ &= \mathrm{H}\left(\tau + \tau_a^{(0)} + \sum_{k=1}^{i-1} \tau_s^{(k)} + \tau_b^{(i_0)} \right). \end{aligned} \tag{B-18}$$

In the latter expression we use Eq. B-11.

Appendix B2: Separability of re-mixed representation theorems

In the Sec. *Marchenko with trivial initial estimate*, we introduced an unknown operator $\mathbf{B}$ to transform the overlap $\boldsymbol{\chi}_+$ between the focusing function $\mathbf{F}_1^+$ and the Green's function $(\mathbf{G}^{-,-})^*$ to a trivial one. Thus, the re-mixed correlation-type representation theorem in Eq. 14 is separable by definition, except for an identity matrix. However, the separability of the re-mixed convolution-type representation theorem in Eq. 13 is not guaranteed and is assessed below.

The re-mixed representation theorem in Eq. 13 is separable if the last event of the re-mixed focusing function $\mathbf{V}_1^-$ arrives at the recording surface before the first event of the re-mixed Green's function $\mathbf{U}^{-,+}$,

$$\tau_\Omega(V_{1,ab}^-) < \tau_\alpha(U_{ab}^{-,+}), \tag{B-19}$$

which can be re-written as,

$$\tau_\Omega(F_{1,as}^-) + \tau_\Omega(B_{sb}) < \tau_\alpha(G_{ap}^{-,+}) + \tau_\alpha(B_{pb}). \tag{B-20}$$

Now, we define the first and last arrival times of the re-mixing operator $\mathbf{B}$. The re-mixing operator projects the Green's function $(\mathbf{G}^{-,-})^*$ onto an identity matrix plus an acausal coda. Hence, the first event of the re-mixing operator coincides with the first event of the inverse $\left((\mathbf{G}^{-,-})^*\right)^{-1}$. For example, the first, but time-reversed, event of B_{ps} is depicted by path V in Fig. 3b. We sum the one-way travel times along this path for an arbitrary component ab,

$$\tau_\alpha(B_{ab}) = \tau_a^{(i_0)} + \sum_{k=1}^{i-1} \tau_p^{(k)} + \tau_b^{(0)}. \tag{B-21}$$

Further, we heuristically assume that the re-mixing operator has the same temporal extent as the overlap $\boldsymbol{\chi}_+$ between the focusing function $\mathbf{F}_1^+$ and the Green's function $(\mathbf{G}^{-,-})^*$, which is $\sum_{k=1}^{i-1} \left(\tau_s^{(k)} - \tau_p^{(k)} \right)$. As a result, the one-way travel time of the last event of the re-mixing operator is,

$$\tau_\Omega(B_{ab}) = \tau_a^{(i_0)} + \sum_{k=1}^{i-1} \tau_s^{(k)} + \tau_b^{(0)}. \tag{B-22}$$

Thorough empirical investigations confirm this result. Upon substituting Eqs. B-6-B-7 and Eqs. B-21-B-22 in Eq. B-20 and using Eq. B-2, we find the $\boldsymbol{\chi}_-^B$-separability-condition for the re-mixed Marchenko scheme,

$$\sum_{k=1}^{i-1} \Delta z^{(k)} \left(s_{z,s}^{(k)} - s_{z,p}^{(k)} \right) < \Delta z^{(i)} s_{z,p}^{(i)}. \tag{B-23}$$

Note that the choice of the level z_i within the i^{th} layer (labelling $i_{0/1}$) was used for the derivation but dropped in the separability conditions in Eqs. B-8, B-12 and B-23.

Now we derive expressions for the re-mixed projectors $\mathbf{P}_B^\pm$. Analogous to the derivation of the separability conditions, we use arrival times of first and last events of specific wavefields to find the re-mixed projectors. From Eqs. 15-16 follows that the re-mixing operator $\mathbf{B}$ unfolds the overlap $\boldsymbol{\chi}_+$ between the focusing function $\mathbf{F}_1^+$ and the Green's function $(\mathbf{G}^{-,-})^*$, except for an identity matrix. In consequence, the diagonal elements of the projector $\mathbf{P}_B^+$ should only preserve positive times, including time zero to account for Eq. 15,

$$P_{B,pp}^+ = P_{B,ss}^+ = \mathrm{H}(\tau). \tag{B-24}$$

The first arrival times of the individual matrix elements, $V_{ab}^+ = F_{1,ac}^+ B_{cb}$, only differ by an a-wave propagation of $F_{1,ac}^+$ and a b-wave propagation of B_{cb}, both through the top layer. Hence, the diagonal elements of the projector $\mathbf{P}_B^+$ in Eq. B-24 can be generalized to an arbitrary projector element,

$$P_{B,ab}^+ = \mathrm{H}\left(\tau + (1 - \delta_{ab}) \Delta z^{(0)} \left(s_{z,a}^{(0)} - s_{z,b}^{(0)} \right) \right), \tag{B-25}$$

where δ_{ab} denotes the Kronecker delta.

Next, we derive an expression for the projector $\mathbf{P}_B^-$. The re-mixing operator is not designed to modify the focusing function $\mathbf{F}_1^-$ or the Green's function $\mathbf{G}^{-,+}$ in a special way. Therefore, in a general case the arrival time of the last event of the re-mixed focusing function $V_{ab}^- = F_{1,ac}^- B_{cb}$ is obtained by adding the last arrival times of the focusing function $F_{1,as}^-$ and the re-mixing operator B_{sb},

$$\begin{aligned} P_{B,ab}^- &= \mathrm{H}\left(\tau - \left[\tau_\Omega\left(F_{1,as}^-\right) + \tau_\Omega\left(B_{sy}\right)\right]\right) \\ &= \mathrm{H}\left(\tau - \Delta z^{(0)}\left(s_{z,a}^{(0)} + s_{z,b}^{(0)}\right) - 2\sum_{k=1}^{i-1}\Delta z^{(k)} s_{z,s}^{(k)}\right), \end{aligned} \tag{B-26}$$

where we used Eqs. B-2, B-6 and B-22.

Although the expressions for the re-mixed projectors might appear complicated, they can be constructed easily from: (1) a smooth P- and S-wave velocity model combined with (2) an estimate of the position of the shallowest reflector and (3) an estimate of the position of the reflector above the redatuming depth. The latter estimate could be obtained e.g. by selecting a redatuming depth below a strong reflector that can be easily localized. Compared to the conventional elastodynamic Marchenko method the required a-priori knowledge is significantly reduced.

Appendix B3: From monotonicity to separability conditions

In this appendix, we quantify the monotonicity assumptions of the ISS as separability conditions.

The monotonicity assumption (i) requires temporal ordering of primaries according to the reflector ordering in depth. Hence, for an arbitrary elastic component of the reflection response, R_{ab}, the slowest primary associated with an interface $j-1$ (at the bottom of layer $j-1$) must reach the recording surface before the fastest primary associated with the next, deeper, interface j (see Fig. 5),

$$\tau_\Omega(R_{ab}^{(j-1)}) < \tau_\alpha(R_{ab}^{(j)}). \tag{B-27}$$

The superscripts refer to (converted) primary reflections associated with the interfaces $j-1$ and j. Now, we sum the travel times along the travel path of these two primaries, leading to,

$$\tau_\Omega(R_{ab}^{(j-1)}) = \tau_a^{(0)} + 2\sum_{k=1}^{j-1}\tau_s^{(k)} + \tau_b^{(0)}, \tag{B-28}$$

and,

$$\tau_\alpha(R_{ab}^{(j)}) = \tau_a^{(0)} + 2\sum_{k=1}^{j}\tau_p^{(k)} + \tau_b^{(0)}. \tag{B-29}$$

Next, we substitute Eqs. B-28 and B-29 in Eq. B-27, replace the travel times by Eq. B-2, and obtain a separability condition,

$$\sum_{k=1}^{j-1}\Delta z^{(k)}\left(s_{z,s}^{(k)} - s_{z,p}^{(k)}\right) < \Delta z^{(j)} s_{z,p}^{(j)}. \tag{B-30}$$

Redatuming from the recording level z_0 to z_i requires that all interfaces between these two depth levels satisfy monotonicity, i.e. Eq. B-30 becomes the separability condition in Eq. 23.

The monotonicity assumption (ii) requires that multiples are recorded after their generating primaries. Hence, for redatuming to the depth level z_i the slowest primary reflection associated with the interface $i-1$ must predate the fastest multiple generated by the same interface,

$$\tau_\Omega\left(R_{ab}^{(i-1)}\right) < \tau_\alpha\left(R_{m,ab}^{(i-1)}\right), \tag{B-31}$$

where $R_{m,ab}^{(i-1)}$ represents the multiples generated by the interface $i-1$. Again, we sum the travel times along the paths of these two events,

$$\tau_\Omega\left(R_{ab}^{(i-1)}\right) = \tau_a^{(0)} + 2\sum_{k=1}^{i-1}\tau_s^{(k)} + \tau_b^{(0)}, \tag{B-32}$$

and,

$$\begin{aligned} &\tau_\alpha\left(R_{m,ab}^{(i-1)}\right) = \\ &\tau_a^{(0)} + 2\sum_{k=1}^{i-1}\tau_p^{(k)} + 2\,\min\left\{\tau_p^{(k)}\middle| k\in[1,i]\right\} + \tau_b^{(0)}. \end{aligned} \tag{B-33}$$

Upon substituting Eqs. B-32 and B-33 in Eq. B-31 and replacing the travel times by Eq. B-2, the monotonicity assumption (ii) can be written as,

$$\sum_{k=1}^{i-1}\Delta z^{(k)}\left(s_{z,s}^{(k)} - s_{z,p}^{(k)}\right) < \min\left\{\Delta z^{(k)} s_{z,p}^{(k)}\middle| k\in[1,i]\right\}, \tag{B-34}$$

which is the separability condition in Eq. 24. Note that, for multiple generators above the interface $i-1$, the condition in Eq. B-34 is relaxed because the left-hand side will remain constant or decrease, while the right-hand side will remain constant or increase.

APPENDIX C: MEDIUM PARAMETERS

This appendix contains the medium parameters used for the experiments shown in Figs. 1-3 (see Tab. C-1 and C-2). Note that the values of the medium parameters are adjusted to ensure all events associated with the horizontal-slowness, $s_x = 2\times10^{-4}\,\mathrm{m}$, are recorded on-sample, i.e. the travel time of each event is an integer-multiple of the temporal sampling interval. The values are within a reasonable range but are not associated with any specific material. We used exaggerated density contrasts to generate strong, well-visible, events. In realistic media the contrasts may be weaker but much more numerous. Hence, there will be many weak, as opposed to a few strong, converted waves. The Marchenko method and the separability conditions are independent of the number and strength of these events, and thus, our analysis can be generalized for more realistic media.

$z(\mathrm{m})$	$c_p(\mathrm{m\,s^{-1}})$	$c_s(\mathrm{m\,s^{-1}})$	$\rho(\mathrm{kg\,m^{-3}})$
-∞ - 500	1993.63	898.38	4200
500 - 1700	1897.78	1099.20	1100
1700 - 2501.07	2500.00	1386.75	6000
2501.07 - ∞	2695.26	1611.32	3500

Table C-1: This table contains the medium parameters used for the experiment shown in Figs. 1 and 2a (for the acoustic experiment the shear wave velocity is set to zero). The focusing depth is at $z_f = 1902.07\,\mathrm{m}$. The experiment shown in Fig. 2b uses the same medium parameters, except that the bottom interface is moved from $z = 2501.07\,\mathrm{m}$ to $z = 2299.00\,\mathrm{m}$.

$z(\mathrm{m})$	$c_p(\mathrm{m\,s^{-1}})$	$c_s(\mathrm{m\,s^{-1}})$	$\rho(\mathrm{kg\,m^{-3}})$
-∞ - 500	1993.63	898.38	1100
500 - 1250.56	2500	1796.05	4200
1250.56 - 1503.15	1505.43	1050.85	1700
1503.15 - 2304.24	1900.00	1006.04	6000
2304.24 - ∞	2695.26	1396.65	3500

Table C-2: This table contains the medium parameters used for the experiment shown in Fig. 3a. The focusing depth is at $z_f = 1703.42\,\mathrm{m}$. The experiment shown in Fig. 3b uses the same medium parameters, except that the second interface from above is moved from $z = 1250.56\,\mathrm{m}$ to $z = 1452.63\,\mathrm{m}$.

APPENDIX D: NUMERICAL EXAMPLE OF THE RE-MIXING OPERATOR

In this appendix, we determine and show the re-mixing operator associated with the experiment in Fig. 6. Since, to our knowledge, the operator $\mathbf{B}$ cannot be computed directly, we obtain it indirectly: Firstly, we retrieve $\mathbf{V}_1^{\pm}$ by solving the re-mixed representation theorems (provided that the $\boldsymbol{\chi}_{-}^{B}$ separability condition in Eq. 22 holds) and model $\mathbf{F}_1^{\pm}$ via wavefield extrapolation. Secondly, we obtain the re-mixing operator $\mathbf{B}$ by solving,

$$\mathbf{V}_1^{\pm} = \mathbf{F}_1^{\pm}\mathbf{B}, \tag{D-1}$$

by deconvolution. We evaluate this deconvolution for up- and downgoing fields independently to confirm that both cases lead to the same solution. The resulting re-mixing operator (see Fig. 7) has a finite duration,

$$\tau_{\Omega}(B_{pp}) - \tau_{\alpha}(B_{pp}) = 0.18\,\mathrm{s}, \tag{D-2}$$

which is equal to the expected one (using Eqs. B-2, B-21 and B-22),

$$\tau_{\Omega}(B_{pp}) - \tau_{\alpha}(B_{pp}) = \sum_{k=1}^{i-1} \Delta z^{(k)} \left(s_{z,s}^{(k)} - s_{z,p}^{(k)} \right). \tag{D-3}$$

Moreover, the re-mixing operator contains a fast multiple at $\tau = \tau_c$, which constructs event C in Fig. 6 via Eq. 26. At zero-incidence, the re-mixing operator simplifies to a single event (see s_x-τ gather in Fig. 7c).

REFERENCES

Amundsen, L., 2001, Elimination of free-surface related multiples without need of the source wavelet: Geophysics, **66**, 327–341.

Bava, G. P., and G. Ghione, 1984, Inverse scattering for optical couplers. Exact solution of Marchenko equations: Journal of Mathematical Physics, **25**, 1900–1904.

Broggini, F., R. Snieder, and K. Wapenaar, 2012, Focusing the wavefield inside an unknown 1D medium: Beyond seismic interferometry: Geophysics, **77**, A25–A28.

Claerbout, J. F., 1985, Imaging the earth's interior: Blackwell scientific publications Oxford.

Coates, R. T., and A. B. Weglein, 1996, Internal multiple attenuation using inverse scattering: Results from prestack 1 & 2D acoustic and elastic synthetics, *in* SEG Technical Program Expanded Abstracts 1996: Society of Exploration Geophysicists, 1522–1525.

de Hoop, A. T., 1995, Handbook of radiation and scattering of waves: Acoustic waves in fluids, elastic waves in solids, electromagnetic waves: Academic Press, London.

Dukalski, M., and K. de Vos, 2017, Marchenko inversion in a strong scattering regime including surface-related multiples: Geophysical Journal International, **212**, 760–776.

———, 2020, A closed formula for true-amplitude overburden-generated interbed de-multiple: 82nd EAGE Conference and Exhibition 2020, 1–5.

Dukalski, M., E. Mariani, and K. de Vos, 2019, Handling short period scattering using augmented Marchenko autofocusing: Geophysical Journal International, **216**, 2129–2133.

El-Emam, A., A. Mohamed, and H. Al-Qallaf, 2001, Multiple attenuation techniques, case studies from Kuwait, *in* SEG Technical Program Expanded Abstracts 2001: Society of Exploration Geophysicists, 1317–1320.

Elison, P., M. Dukalski, K. de Vos, D. van Manen, and J. Robertsson, 2020, Data-driven control over short-period internal multiples in media with a horizontally layered overburden: Geophysical Journal International, **221**, 769–787.

Frasier, C. W., 1970, Discrete time solution of plane P-SV waves in a plane layered medium: Geophysics, **35**, 197–219.

Hubral, P., S. Treitel, and P. R. Gutowski, 1980, A sum autoregressive formula for the reflection response: Geophysics, **45**, 1697–1705.

Jakubowicz, H., 1998, Wave equation prediction and removal of interbed multiples: SEG technical program expanded abstracts 1998, 1527–1530.

Kennett, B. L. N., and N. J. Kerry, 1979, Seismic waves in a stratified half-space: Geophysical Journal International, **57**, 557–583.

Meles, G. A., K. Wapenaar, and J. Thorbecke, 2018, Virtual plane-wave imaging via Marchenko redatuming: Geophysical Journal International, **214**, 508–519.

Mildner, C., M. Dukalski, P. Elison, K. D. Vos, F. Broggini, and J. O. A. Robertsson, 2019, True amplitude-versus-offset Green's function retrieval using augmented Marchenko focusing: Presented at the 81st EAGE Conference and Exhibition 2019.

Nita, B. G., and A. B. Weglein, 2009, Pseudo-depth/intercept-

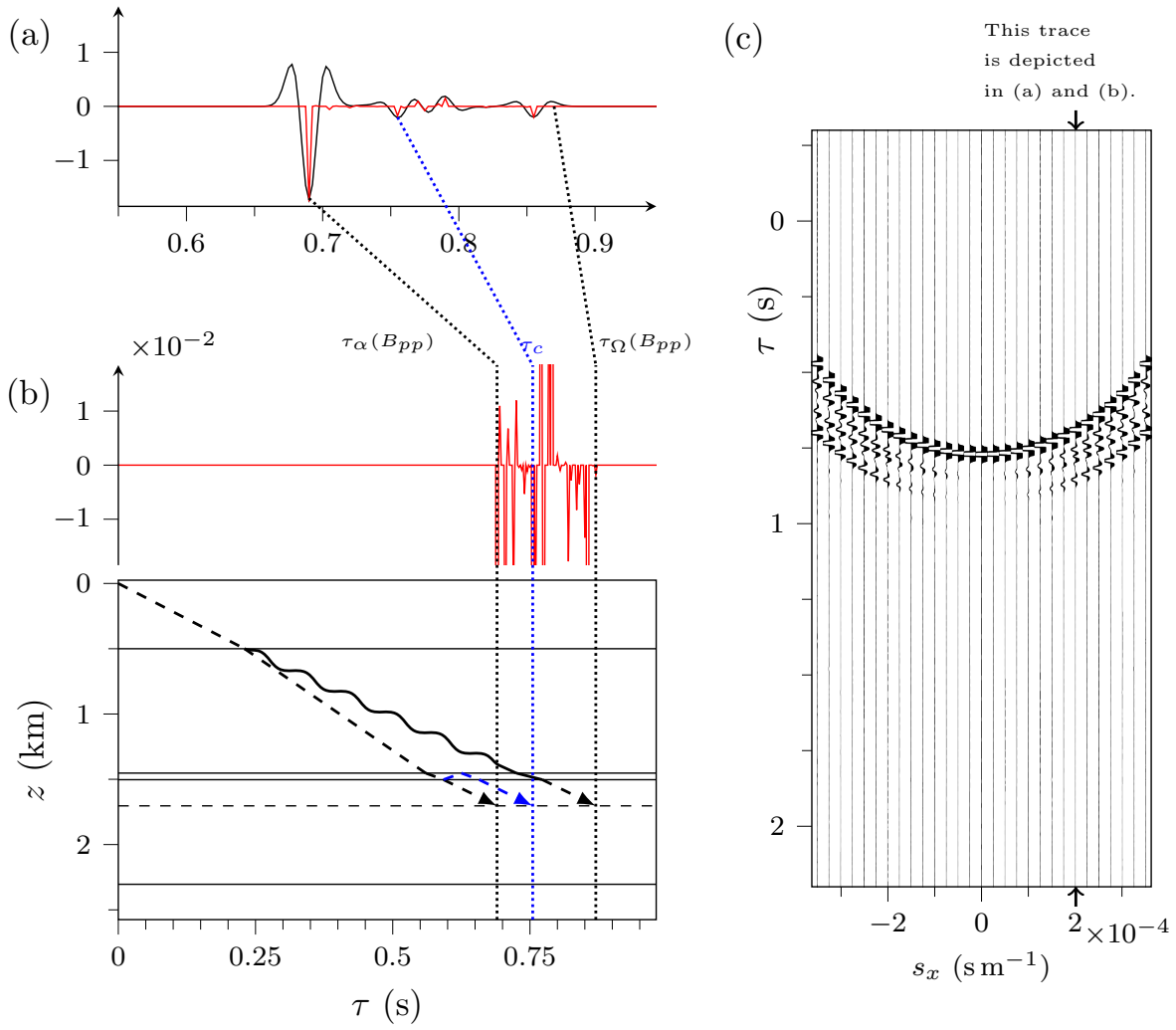

Figure 7: Re-mixing operator $\mathbf{B}$ associated with the numerical example in Fig. 6 (arbitrarily chosen *pp* component). Panel (a) shows the re-mixing operator before (red) and after (black) convolution with a 30 Hz Ricker wavelet. In panel (b) the clipping values of the time and amplitude axes are adjusted to highlight the travel paths associated with three selected events of the re-mixing operator: (1) the first event of B_{pp}, (2) a fast multiple that persists in the de-multiple result (see event C in Fig. 6), and (3) the last event of B_{pp}. Due to its small amplitude, the last event is only visible in panel (b). Dotted lines point to the arrivals associated with the cartoon arrows and label the travel times of these events as $\tau_\alpha(B_{pp})$, τ_c and $\tau_\Omega(B_{pp})$. Again, dashed and sinusoidal lines represent P- and S-waves, respectively. Panel (c) shows an s_x-τ gather of the re-mixing operator (after convolution with a 30 Hz Ricker wavelet). By analyzing all elastic components (not shown here), it can be seen that the operator $\mathbf{B}$ is a scaled and delayed identity plus a small coda. Hence, its determinant is approximately a phase-shift with a non-zero amplitude, meaning that $\mathbf{B}$ is invertible.

time monotonicity requirements in the inverse scattering algorithm for predicting internal multiple reflections: Communications in Computational Physics, **5**, 163.

Ravasi, M., I. Vasconcelos, A. Kritski, A. Curtis, C. A. da Costa Filho, and G. A. Meles, 2016, Target-oriented Marchenko imaging of a North Sea field: Geophysical Journal International, **205**, 99–104.

Reinicke, C., M. Dukalski, and K. Wapenaar, 2019, Do we need elastic internal de-multiple offshore Middle East, or will acoustic Marchenko suffice: Presented at the SEG/KOC Workshop: Seismic Multiples - The Challenges and the Way Forward, Kuwait.

Reinicke, C., G. A. Meles, and K. Wapenaar, 2018, Elastodynamic plane wave Marchenko redatuming: theory and examples: Presented at the 80th EAGE Conference and Exhibition 2018.

Slob, E., K. Wapenaar, F. Broggini, and R. Snieder, 2014, Seismic reflector imaging using internal multiples with Marchenko-type equations: Geophysics, **79**, S63–S76.

Staring, M., R. Pereira, H. Douma, J. van der Neut, and K. Wapenaar, 2018, Source-receiver Marchenko redatuming on field data using an adaptive double-focusing method: Geophysics, **83**, S579–S590.

Sun, J., and K. A. Innanen, 2016, Interbed multiple prediction on land: which technology, and which domain?: Recorder, **41**, 24–29.

———, 2019, A plane-wave formulation and numerical analysis of elastic multicomponent inverse scattering series internal multiple prediction: Geophysics, **84**, V255–V269.

Tunnicliffe-Wilson, G., 1972, The factorization of matricial spectral densities: Siam J. Appl. Math, **23**, 420–426.

Ursin, B., 1983, Review of elastic and electromagnetic wave propagation in horizontally layered media: Geophysics, **48**, 1063–1081.

van der Neut, J., and K. Wapenaar, 2016, Adaptive overburden elimination with the multidimensional Marchenko equation: Geophysics, **81**, T265–T284.

Wapenaar, K., 2014, Single-sided Marchenko focusing of compressional and shear waves: Physical Review E, **90**, 63202.

Wapenaar, K., F. Broggini, E. Slob, and R. Snieder, 2013, Three-dimensional single-sided Marchenko inverse scattering, data-driven focusing, Green's function retrieval, and their mutual relations: Physical Review Letters, **110**, 084301.

Wapenaar, K., and E. Slob, 2015, Initial conditions for elastodynamic Green's function retrieval by the Marchenko method: SEG Technical Program Expanded Abstracts 2015, 5074–5080.

Wapenaar, K., J. Thorbecke, J. van der Neut, F. Broggini, E. Slob, and R. Snieder, 2014, Marchenko imaging: Geophysics, **79**, WA39–WA57.

Ware, J. A., and K. Aki, 1969, Continuous and Discrete Inverse-Scattering Problems in a Stratified Elastic Medium . I . Plane Waves at Normal Incidence: The journal of the Acoustical Society of America, **45**, 911–921.

Weglein, A. B., F. A. Gasparotto, P. M. Carvalho, and R. H. Stott, 1997, An inverse-scattering series method for attenuating multiples in seismic reflection data: Geophysics, **62**, 1975–1989.

Zakharov, V. E., and A. B. Shabat, 1973, Interaction between solitons in a stable medium: Sov. Phys. JETP, **37**, 823–828.